Geological Society of America Bulletin, published online on 30 June 2014 as doi:10.1130/B31038.1

Calibration of a conodont apatite-based Ordovician $^{87}Sr/^{86}Sr$ curve to biostratigraphy and geochronology: Implications for stratigraphic resolution

Matthew R. Saltzman[1,†], Cole T. Edwards[1], Stephen A. Leslie[2], Gary S. Dwyer[3], Jeffrey A. Bauer[4], John E. Repetski[5], Anita G. Harris[5], and Stig M. Bergström[1]

[1]*School of Earth Sciences, Ohio State University, Columbus, Ohio 43210, USA*
[2]*Department of Geology and Environmental Science, James Madison University, Harrisonburg, Virginia 22807, USA*
[3]*Division of Earth and Ocean Sciences, Nicholas School of the Environment, Duke University, Durham, North Carolina 27708, USA*
[4]*Department of Natural Sciences, Shawnee State University, Portsmouth, Ohio 45662, USA*
[5]*U.S. Geological Survey, Reston, Virginia 20192, USA*

ABSTRACT

The Ordovician $^{87}Sr/^{86}Sr$ isotope seawater curve is well established and shows a decreasing trend until the mid-Katian. However, uncertainties in calibration of this curve to biostratigraphy and geochronology have made it difficult to determine how the rates of $^{87}Sr/^{86}Sr$ decrease may have varied, which has implications for both the stratigraphic resolution possible using Sr isotope stratigraphy and efforts to model the effects of Ordovician geologic events. We measured $^{87}Sr/^{86}Sr$ in conodont apatite in North American Ordovician sections that are well studied for conodont biostratigraphy, primarily in Nevada, Oklahoma, the Appalachian region, and Ohio Valley. Our results indicate that conodont apatite may provide an accurate medium for Sr isotope stratigraphy and strengthen previous reports that point toward a significant increase in the rate of fall in seawater $^{87}Sr/^{86}Sr$ during the Middle Ordovician Darriwilian Stage. Our $^{87}Sr/^{86}Sr$ results suggest that Sr isotope stratigraphy will be most useful as a high-resolution tool for global correlation in the mid-Darriwilian to mid-Sandbian, when the maximum rate of fall in $^{87}Sr/^{86}Sr$ is estimated at ~$5.0–10.0 \times 10^{-5}$ per m.y. Variable preservation of conodont elements limits the precision for individual stratigraphic horizons. Replicate conodont analyses from the same sample differ by an average of ~4.0×10^{-5} (the 2σ standard deviation is 6.2×10^{-5}), which in the best case scenario allows for subdivision of Ordovician time intervals characterized by the highest rates of fall in $^{87}Sr/^{86}Sr$ at a maximum resolution of ~0.5–1.0 m.y. Links between the increased rate of fall in $^{87}Sr/^{86}Sr$ beginning in the mid-late Darriwilian (*Phragmodus polonicus* to *Pygodus serra* conodont zones) and geologic events continue to be investigated, but the coincidence with a long-term rise in sea level (Sauk-Tippecanoe megasequence boundary) and tectonic events (Taconic orogeny) in North America provides a plausible explanation for the changing magnitude and $^{87}Sr/^{86}Sr$ of the riverine Sr flux to the oceans.

INTRODUCTION

The strontium isotopic ($^{87}Sr/^{86}Sr$) composition of the ocean is homogeneous at any given time in the geologic past because of the long oceanic residence time of strontium (~2–4 m.y.) relative to oceanic mixing times (~10^3 yr; Elderfield, 1986; Palmer and Edmond, 1989; Veizer, 1989; McArthur, 1994; Davis et al., 2003). Seawater $^{87}Sr/^{86}Sr$ varies over geologic time (Fig. 1A) in response to changes in the magnitude of the riverine Sr flux, the $^{87}Sr/^{86}Sr$ of rock types being weathered on the continents, and the flux of Sr from seafloor hydrothermal weathering (Hodell et al., 1990; Richter et al., 1992; Ingram et al., 1994; Jones et al., 1994; Banner, 2004; Waltham and Gröcke, 2006; Young et al., 2009). Calibration of the $^{87}Sr/^{86}Sr$ curve to biostratigraphy and geochronology makes it possible to use Sr isotope stratigraphy as an independent method to correlate rocks (Burke et al., 1982; McArthur et al., 2001). Sr isotope stratigraphy is commonly applied to Mesozoic and Cenozoic time periods, but efforts in the Paleozoic have been hindered by a lack of abundance of well-preserved materials and uncertainty in stratigraphic correlation or radiometric age uncertainties (Veizer et al., 1997; McArthur and Howath, 2004; McArthur et al., 2012).

The general structure of the $^{87}Sr/^{86}Sr$ seawater curve for the Ordovician Period is well established and shows falling values from ~0.7090 near the base of the Ordovician to a minimum of ~0.7078 in the middle Katian (Denison et al., 1998; Qing et al., 1998; Shields et al., 2003; Young et al., 2009; McArthur et al., 2012; Fig. 1A). However, the extent to which the rate of fall varies during the Ordovician (Fig. 1B) is less well understood, and more intensive Sr isotope sampling is needed from sections that contain index fossils or well-dated volcanic ash beds. The maximum rate of fall in $^{87}Sr/^{86}Sr$ has been estimated at ~$5.0–10.0 \times 10^{-5}$ per m.y. in the Darriwilian and Sandbian Stages of the Middle to Late Ordovician (Shields et al., 2003; Young et al., 2009). These authors linked the high rate of fall to unusual tectonic activity and sea-level changes that affected Ordovician Sr fluxes. Although parts of the Middle to Late Ordovician clearly stand out as periods of anomalously high rates of change in $^{87}Sr/^{86}Sr$ in McArthur et al. (2012) (Fig. 1B), these same authors cautioned that, as with all pre-Cenozoic time intervals, this result should be carefully examined for evidence of time-scale compression (i.e., anomalously large $^{87}Sr/^{86}Sr$ rates of change that are mere artifacts of poorly constrained radiometric age dates or biostratigraphic correlation) before drawing conclusions about causal factors (e.g., Jurassic example in Waltham and Gröcke, 2006; McArthur and Wignall, 2007).

If observed high rates of change in the Middle to Late Ordovician are not drastically diminished with improvements in radiometric age dates and biostratigraphic calibration, this

†E-mail: saltzman.11@osu.edu.

 doi: 10.1130/B31038.1; 12 figures; 1 table; Data Repository item 2014240.

Geological Society of America Bulletin, published online on 30 June 2014 as doi:10.1130/B31038.1

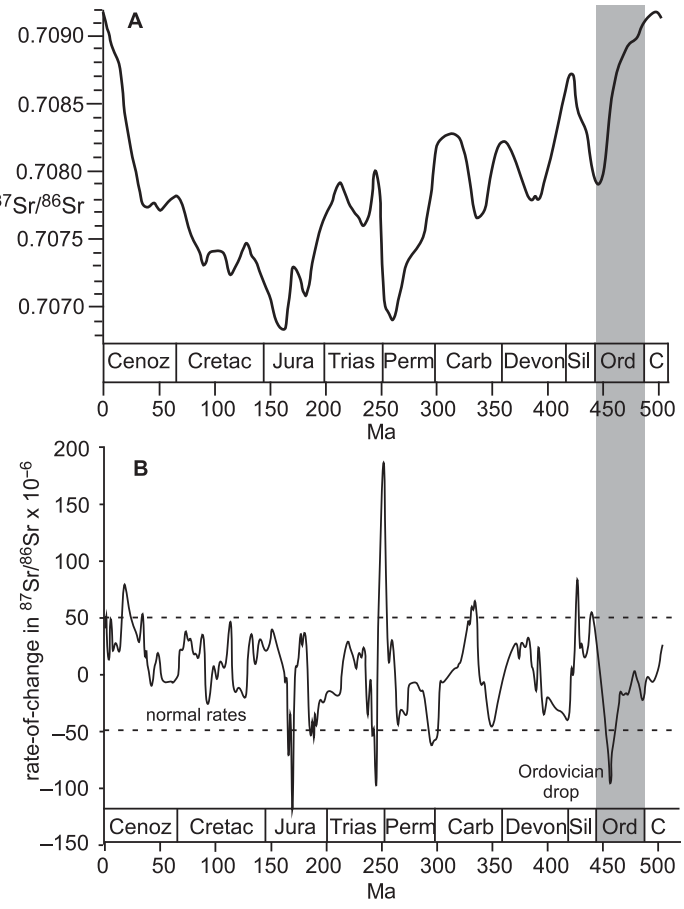

Figure 1. (A) Phanerozoic $^{87}Sr/^{86}Sr$ and (B) rates of change, both after McArthur et al. (2012). The curve in A is the LOWESS (locally weighted scatterplot smoother), which is a statistical nonparametric regression method fit to the data sources in McArthur et al. (2012). Ordovician study interval is highlighted with gray box.

interval, which is marked by major biological and climatic changes (Trotter et al., 2008; Servais et al., 2010), holds great promise for Sr isotope stratigraphy. McArthur et al. (2012) calculated that when rates of $^{87}Sr/^{86}Sr$ change in the Phanerozoic exceed 5.0×10^{-5} per m.y. (Fig. 1B), the stratigraphic resolution in these time periods can theoretically surpass 0.1 m.y. In the Ordovician, 0.1 m.y. resolution using Sr isotope stratigraphy likely cannot be achieved because of limitations in biostratigraphy, geochronology, and sample preservation that result in scatter in $^{87}Sr/^{86}Sr$ data (Shields et al., 2003), and a more reasonable goal is 0.5–1.0 m.y. resolution.

The purpose of this paper is to more accurately calibrate the Ordovician Sr isotope curve to conodont biostratigraphy and geochronology, and to fill in underdocumented parts of the curve. We measured $^{87}Sr/^{86}Sr$ in conodont apatite in North American Ordovician sections that include some of the best studied in the world for conodont biostratigraphy, primarily in Nevada, Oklahoma, the Ohio Valley, and Appalachian region (Figs. 2 and 3). To calculate rates of change in $^{87}Sr/^{86}Sr$, we utilize the new *Geologic Time Scale 2012* (Cooper and Sadler, 2012). Our results, which support use of conodont apatite as an accurate medium for seawater $^{87}Sr/^{86}Sr$ under certain circumstances, strengthen the notion that Ordovician Sr isotope stratigraphy is particularly effective as a high-resolution correlation tool in the mid-Darriwilian to mid-Sandbian Stages characterized by high rates of $^{87}Sr/^{86}Sr$ change at ~$5.0–10.0 \times 10^{-5}$ per m.y.

PRESERVATION OF SEAWATER $^{87}Sr/^{86}Sr$: CONODONTS VS. BRACHIOPODS

The most-detailed investigation of seawater $^{87}Sr/^{86}Sr$ for the Ordovician is the brachiopod-based curve of Shields et al. (2003), which makes up much of the Ordovician data in the Phanerozoic compilation of McArthur et al. (2012) shown in our Figure 1A (note that McArthur et al. [2012] also utilized bulk rock data from Gao and Land, 1991; Denison et al., 1998; Young et al., 2009; and conodont data from Ebneth et al., 2001). Although well-preserved brachiopods composed of diagenetically resistant low-Mg calcite are generally accepted as a medium for accurate measurement of $^{87}Sr/^{86}Sr$ trends in the Ordovician and elsewhere in the Paleozoic (e.g., Korte et al., 2006; Van Geldern et al., 2006; Brand et al., 2012), significant gaps in their availability occur in parts of the Middle to Late Ordovician. Conodont apatite can be extracted from virtually every marine Ordovician-aged carbonate rock and tied to the global conodont biostratigraphic zonation (Fig. 3), which is the most widely used zonation in Ordovician carbonate facies (e.g., Harris et al., 1979; Bergström, 1971, 1986; Sweet, 1984; Sweet et al., 2005; Cooper and Sadler, 2012). The use of conodont apatite as an accurate and precise medium for seawater $^{87}Sr/^{86}Sr$ stratigraphy is debated in the literature because of questions about the commonly observed postmortem incorporation of significant amounts of Sr, which could derive from seawater or non-seawater sources depending on pore-water conditions (e.g., Bertram et al., 1992; Kürschner et al., 1992; Cummins and Elderfield, 1994; Holmden et al., 1996; Ruppel et al., 1996; Ebneth et al., 1997, 2001; Veizer et al., 1997; Qing et al., 1998; Korte et al., 2003, 2004; Martin and Scher, 2004; Twitchett, 2007). Similar debate surrounds use of bulk rock for Sr isotope stratigraphy (e.g., Gao and Land, 1991; Denison et al., 1998; Young et al., 2009), and we have a separate study under way to better characterize accuracy and precision in fossil materials versus bulk rock in the Ordovician using some of the same sections analyzed in the present contribution (Edwards et al., 2013).

Direct comparisons between Ordovician conodonts and brachiopods may be used to assess their accuracy for seawater $^{87}Sr/^{86}Sr$ measurements. The precision (reproducibility) of these materials, which also determines their effectiveness for use in Sr isotope stratigraphy, can be compared with each other but also with younger periods. For example, in the late Neogene replicate analyses of well-preserved foraminiferal calcite could differ by as much as 2.0×10^{-5} (Farrell et al., 1995), and an Early Jurassic $^{87}Sr/^{86}Sr$ study by Jones et al. (1994) found that reproducibility in fossil belemnite and oyster samples was within ~$2.0–2.5 \times 10^{-5}$. This degree of precision, which is close to the external error associated with replicate analyses of the standard (e.g., SRM 987), allows for resolution of small but significant changes in Cenozoic or Mesozoic seawater $^{87}Sr/^{86}Sr$

Geological Society of America Bulletin, published online on 30 June 2014 as doi:10.1130/B31038.1

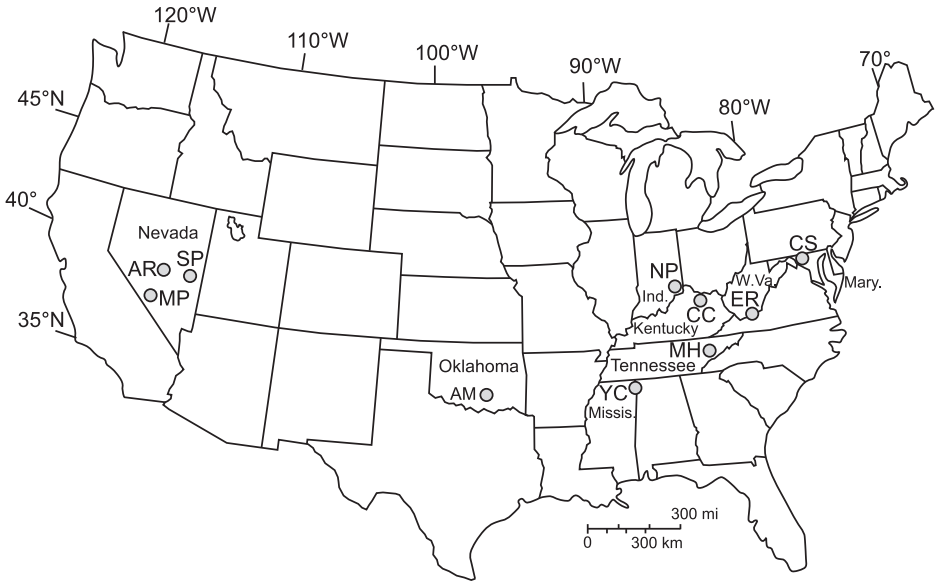

Figure 2. Locality map showing positions of sampled sections in the United States. Abbreviations of study sections as follows: MP—Meiklejohn Peak, AR—Antelope Range, SP—Shingle Pass, AM—Arbuckle Mountains, MH—Marble Hollow, CC—Cominco core, ER—East River Mountain, CS—Clear Spring, NP—New Point, YC—Yellow Creek. Ind—Indiana; Mary—Maryland; W.Va—West Virginia; Missis—Mississippi.

(e.g., ~3.0×10^{-5} across the Cretaceous-Tertiary boundary in MacLeod et al., 2001). In the Paleozoic, a Silurian conodont study by Ruppel et al. (1996) reported precision similar to these Mesozoic and Cenozoic studies (see also Permian conodonts in Needham, 2007), while Diener et al. (1996) reported ~4.0×10^{-5} for Devonian brachiopods (resulting from variables in geological preservation rather than analytical uncertainties). Thus, over geologic time, $^{87}Sr/^{86}Sr$ precision in the analysis of various materials seems to vary between ~2.0 and 4.0×10^{-5} depending on sample preservation and methods (but not including scatter in some data sets that can exceed 10.0×10^{-5} as a result of uncertainty in biostratigraphic correlations used in global compilations; see GSA Data Repository Figure S1 for list of uncertainties[1]).

For conodonts, factors thought to affect seawater $^{87}Sr/^{86}Sr$ preservation are: (1) the rock matrix of the samples from which conodonts are extracted (i.e., shale or limestone), which influences pore-water chemistry and postmortem Sr exchange, (2) thermal alteration, which may also affect Sr exchange and which can be estimated by the conodont alteration index (CAI; Epstein et al., 1977), (3) pretreatment of conodont elements by leaching to remove altered Sr, and (4) the morphology of the conodont elements analyzed, portions of which may be more likely to contain altered Sr. Holmden et al. (1996) proposed that conodont elements embedded in limestone were most likely to preserve seawater $^{87}Sr/^{86}Sr$ values because the Sr incorporated into apatite during early and late diagenesis would be derived originally from seawater (as opposed to diffusion of radiogenic Sr from shale or clay-rich successions; see also the study of fish teeth by Martin and Scher, 2004). Consistent with this notion, conodont elements embedded in a relatively clean matrix such as pure limestone show similar $^{87}Sr/^{86}Sr$ values to co-occurring brachiopods, whereas conodonts extracted from shale-rich horizons are on average 5.0×10^{-5} more radiogenic than brachiopods (Diener et al., 1996; Ebneth et al., 1997).

Bertram et al. (1992) found that conodont elements with CAI below 2.5 were suitable for Sr isotope stratigraphy, whereas a CAI of 4.0 could alter $^{87}Sr/^{86}Sr$ to more radiogenic values by ~1.5×10^{-4} (see also Cummins and Elderfield, 1994; Holmden et al., 1996; Veizer et al., 1997; Woodard et al., 2013). However, Holmden et al. (1996) argued that even at low CAI, a conodont could still be altered because the Sr concentration and $^{87}Sr/^{86}Sr$ of diagenetic fluids appear to be more significant variables (e.g., samples taken from shales impart a high $^{87}Sr/^{86}Sr$ signature during early diagenesis regardless of CAI).

Ruppel et al. (1996) reported that leaching Silurian conodonts in weak acid (see also Martin and Macdougall, 1995; Holmden et al., 1996) could help ensure accurate measurement of $^{87}Sr/^{86}Sr$, and their data fit well with the seawater curve derived from brachiopod calcite (Azmy et al., 1999; Cramer et al., 2011). However, some authors found that leaching may have an insignificant effect on measured $^{87}Sr/^{86}Sr$ in conodonts (John et al., 2008) or that it is not always clear how much leaching is appropriate in biogenic apatite (e.g., see study of fish teeth by Dufour et al., 2007), and thus leaching may be impractical for studies using small initial sample weights of conodont elements. If, as shown by some authors, portions of the conodont element above the base (i.e., crown material or "cusps") have the least altered (least radiogenic) $^{87}Sr/^{86}Sr$ values (Holmden et al., 1996; Trotter et al., 1999), then careful selection of conodont elements is good practice where leaching is impractical.

GEOLOGIC BACKGROUND

Conodont Biostratigraphy

The most widely used fossils for biostratigraphic correlation in the Ordovician are the graptolites and conodonts (Cooper and Sadler, 2012). Graptolites are typically found in shale representing outer-shelf and slope regions of the continental margin, whereas conodonts are abundant in carbonate platform environments. Conodonts were distributed into two biogeographic realms in the Ordovician, known as the North American Midcontinent realm and the North Atlantic realm, which provide parallel zonations for use in biostratigraphy (Sweet and Bergström, 1976, 1984; Webby et al., 2004). Conodonts assigned to the North American Midcontinent realm are generally associated with low-latitude, warm-water environments (Leslie and Lehnert, 2005), whereas North Atlantic realm conodonts occurred in higher latitudes or deeper-water regions with cooler water temperature. In some sections where both shallow- and deeper-water facies are present, both the North American Midcontinent and North Atlantic faunas are found (Harris et al., 1979). In these instances, the method for establishing time equivalence of these parallel zonations can be straightforward. However, in some parts of the Ordovician, the evidence for equating the parallel zonations is indirect.

Geochronology

The Ordovician time scale was recently revised by Cooper and Sadler (2012), who used all available high-quality radiogenic isotope dates to interpolate stage boundary ages (16 dates total

[1]GSA Data Repository item 2014240, data tables, rates of change, conodont images, and figures, is available at http://www.geosociety.org/pubs/ft2014.htm or by request to editing@geosociety.org.

Geological Society of America Bulletin, published online on 30 June 2014 as doi:10.1130/B31038.1

were reappraised and utilized, 11 of which were originally reported by Tucker and McKerrow, 1995). Important new high-precision U-Pb dates not included in Cooper and Sadler (2012) were reported by Sell et al. (2011), Thompson et al. (2012), Leslie et al. (2012), and Sell et al. (2013). These new dates generally support the time scale by Cooper and Sadler (2012), including a ca. 453 Ma age for the Sandbian-Katian boundary (Sell et al. 2013), 459 Ma age for the Darriwilian-Sandbian boundary (Leslie et al., 2012), and a 464 Ma age for the middle Darriwilian (Sell et al., 2011). The excellent ages of Thompson et al. (2012) also appear to support the time scale by Cooper and Sadler (2012), but there is uncertainty in positions of volcanic ash beds (Talacasto and Cerro La Chilca sections) relative to conodont sample horizons in the San Juan Formation (Albanesi et al., 2013). It may be possible to use $\delta^{13}C_{carb}$ calibrated to biostratigraphy (e.g., Edwards and Saltzman, 2014) to refine our understanding of how these new age dates affect the Ordovician time scale of Cooper and Sadler (2012).

METHODS

Study Areas

Oklahoma

The Arbuckle Mountains of Oklahoma contain a nearly complete Ordovician succession (Figs. 2 and 3). Due to shallow burial history, the CAI is very low (~1), indicating minimal thermal alteration. Our conodont samples come from the thick Lower Ordovician carbonates of the Arbuckle Group exposed at the Chapman Ranch section and along Interstate 35 (Dwyer, 1996), and the Middle to Late Ordovician mixed carbonate and siliciclastic rock of the Simpson Group exposed along Interstate 35 (Derby et al., 1991). Conodont abundances are relatively low in the Arbuckle Group (Derby et al., 1991), but they are among the highest in the world in parts of the Simpson Group (Bauer, 1987, 2010).

Key zonal index fossils found in the Middle to Late Ordovician portion of the Simpson Group include species of *Histiodella* (*Histiodella altifrons*, *Histiodella sinuosa*, *Histiodella holodentata*) in the Joins and Oil Creek Formations (Bauer, 1983, 1987a, 1987b, 1989, 1990, 1994, 2010). The lower part of the McLish contains the index fossils *Phragmodus polonicus* and *Eoplacognathus foliaceus*, and the upper McLish, Tulip Creek, and lower Bromide Formations yield species of *Cahabagnathus* (*Cahabagnathus friendsvillensis* and *Cahabagnathus sweeti*) followed by species of *Baltoniodus* (*Baltoniodus gerdae*) in the upper part of the Bromide Formation.

Figure 3 (*on following page*). Conodont zones and stages of the Ordovician using the *Geologic Time Scale 2012* (for full genus and species names, see Cooper and Sadler, 2012). The conodont zones are represented in formations shown for individual sections in Oklahoma, Nevada, the Appalachian region (Maryland, West Virginia [WV], Tennessee [TN], and Mississippi [MS]), and Ohio Valley (Indiana and Kentucky [IN-KY]). See Figure 2 for study locations and abbreviations of sections, and see text for complete list of references to conodont studies of individual sections and regions. Fill pattern between Knox Group and Wells Creek Formation in Mississippi represents missing section at the Knox unconformity (Dwyer and Repetski, 2012). Full conodont genus and species abbreviations as follows: *Iapetognathus fluctivagus*, *Cordylodus angulatus*, *Rossodus manitouensis*, *Macerodus dianae*, *Acodus deltatus*, *Oepikodus communis*, *Reutterodus andinus*, *Neomultioistodus compressus–Tricladiodus clypeus, Histiodella altifrons*, *Histiodella sinuosa*, *Eoplacognathus variabilis*, *Histiodella holodentata*, *Eoplacognathus suecicus*, *Phragmodus polonicus*, *Pygodus serra*, *Cahabagnathus friendsvillensis*, *Pygodus anserinus*, *Cahabagnathus sweeti*, *Baltoniodus variabilis*, *Plectodina aculeata*, *Erismodus quadridactylus*, *Baltoniodus gerdae*, *Belodina compressa*, *Baltoniodus alobatus*, *Phragmodus undatus*, *Plectodina tenuis*, *Belodina confluens*, *Oulodus velicuspus*, *Oulodus robustus*, *Amorphognathus superbus*, *Amorphognathus ordovicicus*, *Aphelognathus grandis*, *Aphelognathus divergens*, *Aphelognathus shatzeri*.

Nevada

Several sections in Nevada contain nearly complete successions of Ordovician carbonate (Figs. 2 and 3), broken up only by the Eureka Quartzite in parts of the Middle to Late Ordovician (Ethington and Clark, 1981; Harris et al., 1979; Sweet and Tolbert, 1997; Saltzman, 2005). We made a composite of a section at Shingle Pass (eastern Nevada) for the Early to Middle Ordovician (Edwards and Saltzman, 2014) and the Antelope Range (central Nevada) for the Middle and Late Ordovician (Saltzman and Young, 2005). In addition, we supplemented this composite with a partially overlapping curve from Meiklejohn Peak (western Nevada). The overall thermal maturation of individual conodont elements in Nevada ranges from low to relatively high in terms of the CAI (Harris et al., 1979), with amber-colored conodonts from the Antelope Range at ~1 but higher values of 4–5 at Shingle Pass and Meiklejohn Peak.

Key zonal index fossils found in the Middle to Late Ordovician portion of the Shingle Pass section include species of *Histiodella* (*H. altifrons, H. sinuosa*) in the upper Shingle and lower Kanosh Formations (Sweet and Tolbert, 1997; Sweet et al., 2005). The remaining Kanosh and Lehman Formations up to the base of the Eureka Quartzite likely represent the *H. holodentata* and *P. polonicus* zones, based in part on correlations to the nearby Ibex area (Ethington and Clark, 1981; Sweet and Tolbert, 1997; Miller et al., 2003, 2012; Edwards and Saltzman, 2014). In the Antelope Range, our section begins in the upper part of the Antelope Valley Limestone, which contains *H. holodentata*, followed by *E. foliaceus*, *C. friendsvillensis* (Sweet et al., 2005), and *Pygodus serra* (Harris et al., 1979). Above the sandstone at the base of the Copenhagen Formation in the Antelope Range, the index fossils *C. sweeti*, *Pygodus anserinus*, *Eoplacognathus elongatus*, *Baltoniodus gerdae*, *Phragmodus undatus*, and *Phragmodus tenuis* are present beneath the Eureka Quartzite (Saltzman and Young, 2005). Although the time period represented by the *P. polonicus* zone is likely present in the Antelope Range (between horizons with *H. holodentata* and *C. friendsvillensis*), the zonal index fossil is absent; at Meiklejohn Peak, both *P. polonicus* and the North Atlantic equivalent index fossil *Eoplacognathus suecicus* are present (Harris et al., 1979; Sweet et al., 2005).

Appalachian Region (Maryland, Tennessee, Mississippi, and West Virginia)

The Clear Spring, Maryland, section contains a nearly complete Dapingian to Sandbian succession exposed in a road cut along Interstate 70 (Brezinski, 1996; Leslie et al., 2011), which includes the upper part of the Rockdale Run Formation, the Pinesburg Station Dolomite, the St. Paul Group (Row Park and New Market Formations), and the Chambersburg Formation (Figs. 2 and 3). The CAI is relatively high at ~4. Our conodont samples yielded Sandbian index fossils *B. gerdae* and *Belodina compressa* in the Chambersburg Formation but no conodonts that are useful for high-resolution biostratigraphy in the older formations. For these older formations, we utilized conodont range data from nearby pasture exposures studied by Boger (1976), which yielded *C. friendsvillensis* in the lower St. Paul, and a section ~3.5 km along strike in the Chesapeake and Ohio Canal National Park that yielded *H. altifrons* in the upper Rockdale Run (Sando, 1957; Brezinski et al., 1999, 2012).

Geological Society of America Bulletin, published online on 30 June 2014 as doi:10.1130/B31038.1

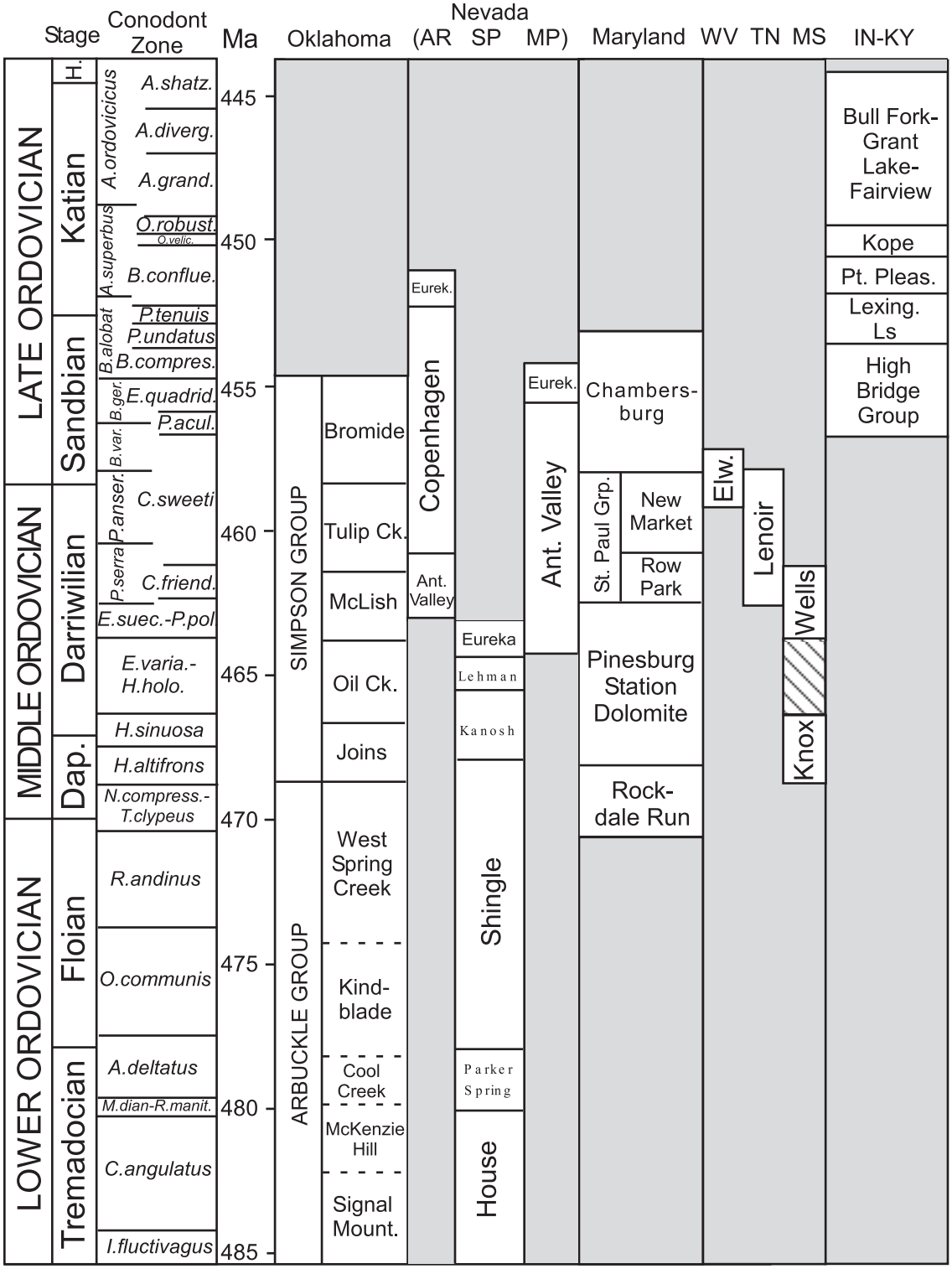

Because of the restricted, shallow-water facies that dominate the Middle Ordovician at Clear Spring (Neuman, 1951; Mitchell, 1982, 1985), the section at Marble Hollow in Tennessee (Figs. 2 and 3) was also analyzed to provide detailed coverage in the late Darriwilian *P. serra–C. friendsvillensis* and *P. anserinus–C. sweeti* zones, which capture the important transition to higher rates of $^{87}Sr/^{86}Sr$ fall (Fig. 1). The Marble Hollow section (CAI ~4) is also important in that it was sampled densely enough for conodonts to capture the evolutionary transition between the *P. serra* and *P. anserinus* zones within a few meters of section (Bergström, 1973). The Yellow Creek core in Mississippi (Figs. 2 and 3) spans the *H. altifrons* through *C. friendsvillensis* zones, including the interval of the Knox unconformity marked by removal of

Geological Society of America Bulletin, published online on 30 June 2014 as doi:10.1130/B31038.1

the *H. holodentata* zone (Dwyer and Repetski, 2012). The section at East River Mountain, West Virginia (Figs. 2 and 3), is included here because of the presence of a volcanic ash bed dated to 458.7 Ma (uncertainty <0.5 m.y.; Leslie et al., 2012) that lies just below a conodont sample analyzed for $^{87}Sr/^{86}Sr$.

Ohio Valley Midcontinent Region (Kentucky, Indiana)

The Cominco core (also known as the Minerva core, or section 70ZA), drilled in northern Kentucky, contains a nearly complete Late Ordovician (Sandbian-Katian) succession (Figs. 2 and 3; Sweet, 1984; Dwyer, 1996). The Cominco core is the formal standard reference section (SRS) for graphic correlation of the Late Ordovician (Votaw, 1971; Sweet, 1984, 1995), and the species that Sweet (1984) used to name conodont-based chronozones, including *Plectodina aculeata*, *B. compressa*, *P. undatus*, *P. tenuis*, *Belodina confluens*, *Oulodus velicuspis*, and *Oulodus robustus*, are present in this core. The New Point core from eastern Indiana partially overlaps the Cominco core and is used to extend our $^{87}Sr/^{86}Sr$ data set to near the top of the Ordovician, including the *Aphelognathus grandis* zone (and possibly *Aphelognathus divergens* and *Aphelognathus shatzeri* zones; Dwyer, 1996; Figs. 2 and 3). In both the Cominco and New Point cores, the CAI is ~1.

Conodont Apatite Sample Materials, Preparation and Analysis

Ohio State University

Conodonts were obtained from carbonate rock samples using traditional extraction techniques, using a weak acetic acid (10%–15%) for limestone dissolution and a formic acid solution (6%) buffered with $CaCO_3$ and $Ca(PO_4)_3$ for dolomitic lithologies (see Jeppsson and Anehus, 1995). Between 0.1–0.7 mg samples of whole and broken elements (simple cones, denticulate blades, and ramiform elements with low proportions of basal material; see Holmden et al., 1996; Trotter et al., 1999) were picked that exhibited no visible signs of alteration and were free of mineral overgrowths (see Fig. S2A–S2C for representative photos of Antelope Range, Nevada, conodonts [see footnote 1]). Samples were rinsed with 1 mL of 18 Ω Milli-Q water, sonicated, and left overnight to remove surficial particles or adhesive from slides. Cleaned elements were further treated with ultrapure 1 *M* ammonium acetate (buffered to a pH = 8). A subset of samples was then leached in 0.5 mL of 0.5% acetic acid for 12 h (e.g., Ruppel et al., 1996; Holmden et al., 1996; Needham, 2007; John et al., 2008). After pretreatment, all conodont elements in this study were dissolved in ultrapure 6 *N* HCl, spiked with an ^{84}Sr tracer, and purified using H^+ cation exchange resin via two elutions of 2 *N* HCl through silica glass columns (cf. Foland and Allen, 1991).

The $^{87}Sr/^{86}Sr$ was measured using dynamic multicollection on a Finnigan MAT-261A thermal ionization mass spectrometer at the Radiogenic Isotope Laboratory in the School of Earth Sciences at Ohio State University. Typical intrarun precision was 0.000009 (2σ s.d.). The long-term laboratory value of 67 measurements of the SRM 987 standard over the duration of measurements for this study was $^{87}Sr/^{86}Sr$ = 0.710224 ± 0.000030 (2σ s.d.). The $^{87}Sr/^{86}Sr$ values were normalized for instrumental fractionation using a normal Sr ratio of $^{86}Sr/^{88}Sr$ = 0.119400.

University of North Carolina (See Dwyer, 1996)

Conodonts were ultrasonically cleaned for 10 min in deionized water and dissolved completely in 0.5 mL of 5 *N* nitric acid, and Sr was extracted for isotopic analysis using Sr-Spec cation-exchange resin and procedures modified from those described in Horwitz et al. (1992). Samples were analyzed on a VG Sector 54 multiple collector mass spectrometer at the Department of Geological Sciences, University of North Carolina–Chapel Hill. Typical intrarun precision was 0.000007 (2σ s.d.). The long-term laboratory value of the SRM 987 standard over the duration of measurements for this study was $^{87}Sr/^{86}Sr$ = 0.710267 ± 0.000028 (2σ; *n* = 57). The $^{87}Sr/^{86}Sr$ values were normalized for instrumental fractionation using a normal Sr ratio of $^{86}Sr/^{88}Sr$ = 0.119400.

Interlaboratory Comparison

A set of five Sr samples analyzed at Ohio State were subsequently taken to Duke University (current home institution of G. Dwyer) to be analyzed from the same Teflon beakers (plenty of Sr remained in the beaker from the original conodont dissolution) for interlaboratory comparison of measured $^{87}Sr/^{86}Sr$ (GSA Data Repository Table S3 [see footnote 1]). National Bureau of Standards (NBS) SRM 987 yielded an average $^{87}Sr/^{86}Sr$ value at Duke that was ~4.0×10^{-5} higher than the long-term value at Ohio State. Analyses of the same Sr samples at Duke were higher than those analyzed at Ohio State by between ~2.0 and 4.0×10^{-5} (average was 2.8×10^{-5}) in four of the five samples, consistent with the interlaboratory difference in SRM 987 (1 of the five samples analyzed was actually 2.2×10^{-5} lower at Duke, which may be an artifact of sample transfer, loading, or other variables).

RESULTS

We first report $^{87}Sr/^{86}Sr$ trends (and Sr concentrations where available) in each study section, and then we provide data on the overall precision based on duplicate sample analysis. All $^{87}Sr/^{86}Sr$ values are shown in GSA Data Repository Table S1 (see footnote 1). In Figures 4–10, the $^{87}Sr/^{86}Sr$ values plotted are not corrected for interlaboratory bias (i.e., they have not yet been normalized to a preferred value for the SRM 987 standard because such a correction of ~2×10^{-5} falls within the size of our plotted data symbols). We only normalized our $^{87}Sr/^{86}Sr$ values to an assumed value of 0.710245 for SRM 987 to make the composite curves plotted in Figures 11–12, which required merging data sets from laboratories at Ohio State University (by adding 2.1×10^{-5} to all samples) and University of North Carolina (by subtracting 2.4×10^{-5} from all samples) that differed in values obtained for the SRM 987 standard (see Discussion section; GSA Data Repository Tables S1 and S3 [see footnote 1]).

$^{87}Sr/^{86}Sr$ Curves for Each Section

Oklahoma

In the Arbuckle and Simpson Groups, $^{87}Sr/^{86}Sr$ falls from ~0.7090 to 0.7081 (Figs. 4 and 5). Most of the $^{87}Sr/^{86}Sr$ drop interval in the Simpson Group is concentrated in the upper McLish through Bromide Formations, which corresponds to the *C. friendsvillensis*, *C. sweeti*, *P. aculeate*, and *Erismodus quadridactylus* Midcontinent conodont zones and the *P. serra*, *P. anserinus*, *Baltoniodus variabilis*, and *Baltoniodus gerdae* North Atlantic conodont zones. The average Sr concentration was 12,314 ppm (1σ s.d. is 4605) for the Simpson Group conodont samples (run at Ohio State University) and 14,842 ppm (1σ s.d. 6346) for the Arbuckle Group and lowermost Simpson (run at University of North Carolina).

Nevada

At Shingle Pass, $^{87}Sr/^{86}Sr$ falls from 0.7090 in the House Formation to ~0.7087 in the Lehman Formation (Fig. 6). In the Antelope Range, $^{87}Sr/^{86}Sr$ falls from ~0.7087 in the Antelope Valley Limestone to 0.7079 at the top of the Copenhagen Formation (Figs. 6 and 7). The drop in the Antelope Range begins in about the *P. serra* or *C. friendsvillensis* conodont zones and continues through the *B. gerdae* zone. At Meiklejohn Peak (Fig. 8), which partially overlaps the upper part of the Shingle Pass section and lower-middle Antelope Range section, $^{87}Sr/^{86}Sr$ falls from ~0.7087 in the Antelope Valley Limestone (*P. polonicus–E. suecicus* zones) to 0.7084 just

Geological Society of America Bulletin, published online on 30 June 2014 as doi:10.1130/B31038.1

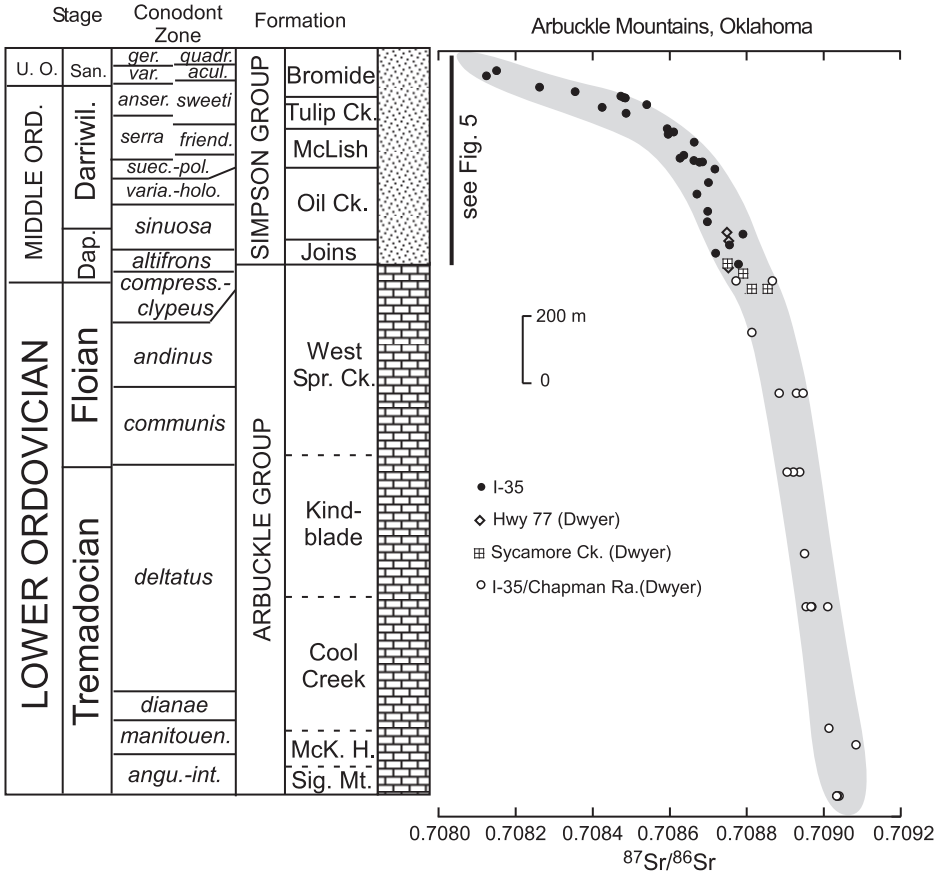

Figure 4. $^{87}Sr/^{86}Sr$ for the Arbuckle Mountains composite, Oklahoma. Data are a composite from four measured sections, three of which are described in detail in Dwyer (1996), and the fourth (I-35, filled circles) is based on Simpson Group samples studied for conodonts in Bauer (1987, 1990, 1994, 2010). See Figure 3 and Cooper and Sadler (2012) for list of conodont zones used. The $^{87}Sr/^{86}Sr$ data shown are not corrected to a common standard and represent the values from individual analyses measured at Ohio State University and the University of North Carolina (see GSA Data Repository Tables S1 and S3 [see text footnote 1]). Any correction needed to account for interlaboratory differences in $^{87}Sr/^{86}Sr$ measurements would be small and approximately the size of the symbols used here (lowering $^{87}Sr/^{86}Sr$ in Dwyer samples and raising them in I-35 data from Ohio State; see text for discussion). The width of the gray band through the data is a qualitative approximation of the overall trend, which is limited by the reproducibility of individual $^{87}Sr/^{86}Sr$ measurements. Some authors have drawn lines through the least radiogenic samples as the best estimate of the seawater $^{87}Sr/^{86}Sr$ trend, but this practice is based on assumptions about diagenetic fluid composition, which has led others to advocate use of a statistical nonparametric regression method to fit the calibration line (e.g., LOWESS fit of McArthur et al., 2012). The vertical bar next to Simpson Group indicates that these same data are plotted in greater detail in Figure 5 in order to show how the $^{87}Sr/^{86}Sr$ values line up against actual conodont species ranges. The lithologies shown are generalized and meant to differentiate rock units within a measured section. Mck. H.—Mckenzie Hill; Sig. Mt.—Signal Mountain. For conodont genera, see Figure 3 caption.

below the Eureka Quartzite (*B. gerdae* zone). Sr concentration averages and standard deviations for Shingle Pass conodont samples are 15,964 ppm (1σ s.d. 4215), 10,165 ppm (1σ s.d. 4215) for the Antelope Range, and 7483 ppm (1σ s.d. 2003) for Meiklejohn Peak.

Appalachian Region (Maryland, Tennessee, Mississippi, and West Virginia)

At Clear Spring, Maryland, $^{87}Sr/^{86}Sr$ falls from ~0.7087 in the Rockdale Run Formation to 0.7082 in the Chambersburg Formation, with most of the drop interval confined to the St. Paul Group in the *C. friendsvillensis*, *C. sweeti*, and *B. gerdae* conodont zones (Fig. 9; see Table S2 and Fig. S3 for consistent results from Boger's [1976] conodonts in nearby sections in Maryland [see footnote 1]). At Marble Hollow, Tennessee (Fig. S4 [see footnote 1]), $^{87}Sr/^{86}Sr$ falls from ~0.7086 (note that the lowest sample is likely altered) to 0.7085 in the Lenoir Formation spanning the *C. friendsvillensis* and *C. sweeti* Midcontinent conodont zones and the *P. serra* and *P. anserinus* North Atlantic zones. In the Yellow Creek core, Mississippi (Fig. S5 [see footnote 1]), values fall from between 0.7088 and 0.7087 in the *H. altifrons* and *H. sinuosa* zones to ~0.7086 in the *C. friendsvillensis* zone (note that the interval of the Knox unconformity is marked by removal of the intervening *H. holodentata* zone; Dwyer and Repetski, 2012). At East River Mountain, West Virginia (Fig. S6 [see footnote 1]), a single sample has a value of ~0.7083 at a horizon just above a K-bentonite bed dated at 458.8 Ma (Leslie et al., 2012). Sr concentrations average 9170 ppm for the Clear Spring conodont samples (1σ s.d. 3826).

Ohio Valley, Midcontinent Region (Kentucky, Indiana)

In the Cominco core, Kentucky, $^{87}Sr/^{86}Sr$ falls from ~0.7083 in the Camp Nelson Formation (beginning in the *P. aculeata* zone) to 0.7079 in the Fairview Formation (possibly as young as *A. robustus* zone) (Fig. 10). The New Point Core (Fig. S7 [see footnote 1]) shows steady values at ~0.7079 to approximately the late Katian. Sr concentrations average 7832 ppm for the Cominco core conodont samples (1σ s.d. 3559).

Sample Precision (Reproducibility)

The $^{87}Sr/^{86}Sr$ analyses of conodont splits from the same rock sample have been performed to report the precision based on reproducibility. For each of the 24 sample splits, between 2 and 4 replicates were run (see GSA Data Repository Table S4 [see footnote 1]). For all the replicate sample sets analyzed, the total difference between the $^{87}Sr/^{86}Sr$ values was as low as 0 to as high as 10.2×10^{-5}; the average difference was 4.0×10^{-5}, and the standard deviation (1σ) was 3.1×10^{-5}.

Reproducibility in conodont $^{87}Sr/^{86}Sr$ can also potentially be evaluated using stratigraphically adjacent samples (i.e., if it can be assumed that the time difference between two adjacent samples is short enough to impart a negligible change from the seawater $^{87}Sr/^{86}Sr$ trend). For example, in the lower McLish Formation, samples separated by 5 m differed by 2.3×10^{-5}, and in the Bromide Formation, several sets of

Geological Society of America Bulletin, published online on 30 June 2014 as doi:10.1130/B31038.1

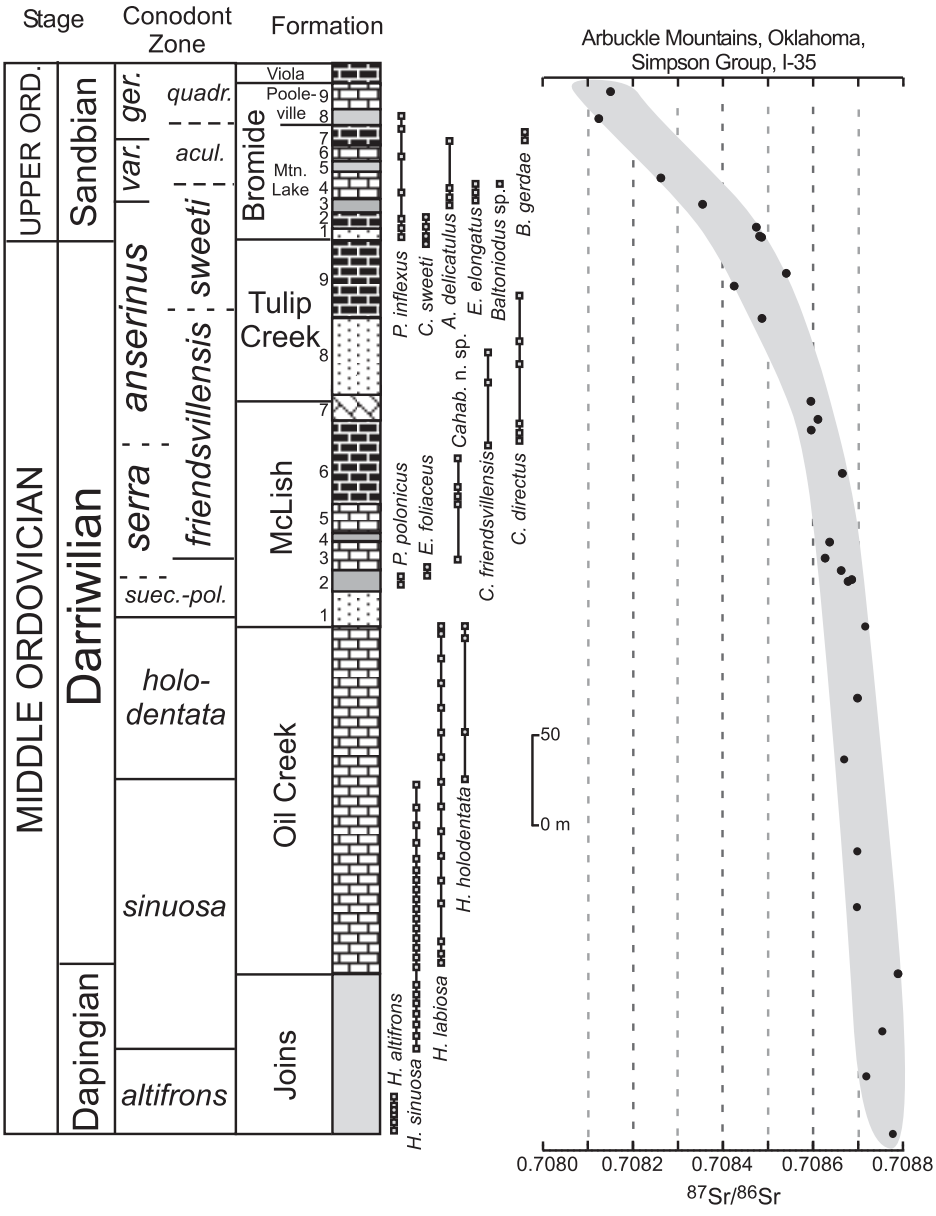

Figure 5. $^{87}Sr/^{86}Sr$ for the I-35 section of the Simpson Group (Joins through Bromide Formations) in the Arbuckle Mountains, Oklahoma (see filled circles in Fig. 4) together with conodont species range data (individual horizons indicated by filled squares; see Bauer, 1987, 1990, 1994, 2010). See Figure 3 and Cooper and Sadler (2012) for list of conodont zones used and abbreviations. See also studies by Bauer (1987, 1990, 1994, 2010) for significance of lithologic subdivisions (numbers 1–9 in both McLish–Tulip Creek, and Bromide). The gray band through the data and lithologic symbols used are generalized (see complete explanation in Fig. 4 caption). For conodont genera, see Figure 3 caption.

samples separated by 5 m differed by 0.8–1.2 × 10^{-5} (Figs. 4 and 5). The largest $^{87}Sr/^{86}Sr$ difference was found in the upper Tulip Creek where two samples separated by 7 m differed by 11.6 × 10^{-5}. In general, there appears to be greater $^{87}Sr/^{86}Sr$ dispersion (lower precision) at higher CAI. For example, in Nevada at Shingle Pass and Meiklejohn Peak (high CAI ~4–5 for both sections), stratigraphically adjacent samples differed by 4.2–11.3 × 10^{-5}, whereas in the Antelope Range (CAI of ~1) samples separated by 2.5 m in the Antelope Valley Limestone differed by 0.9–3.1 × 10^{-5} (Figs. 6–8).

Lastly, the effect of preleaching conodonts with 0.5% acetic acid (e.g., Ruppel et al., 1996; Holmden et al., 1996; Needham, 2007; John et al., 2008) was examined on a small subset of samples in an attempt to evaluate the significance for precision. Although the observed difference between leached residuum and unleached samples was typically less than or equal to our reproducibility based on replicate analyses (discussed already), unfortunately our analytical uncertainty was deemed too high because of the low concentrations of Sr in our leaches to draw any robust conclusions at this time. The $^{87}Sr/^{86}Sr$ analysis on the TIMS at Ohio State University was limited by sample size in that we required at least 0.1 mg of conodont elements but generally aimed for 0.5–0.7 mg. (Note that although we did not preleach all samples in acetic acid, we did preleach all samples in ammonium acetate, which did not reduce sample size.) While our preliminary data are consistent with John et al. (2008), who reported a negligible effect from preleaching, future studies using larger conodont samples are clearly needed (Edwards et al., 2013). Even in cases where leaching is likely to be helpful in conodonts (i.e., where Sr from detrital phases are known to have been incorporated during syndepositional and early diagenesis), there is still uncertainty regarding how much leaching is required (for study of fish teeth, see Dufour et al., 2007).

DISCUSSION

Our results provide a detailed conodont-based Sr isotope curve for most of the Ordovician Period, and in Figure 11 we compile all of our $^{87}Sr/^{86}Sr$ data versus time. We first discuss the preservation of primary seawater $^{87}Sr/^{86}Sr$ values in our conodont apatite-based curve. We then address the stratigraphic resolution possible using $^{87}Sr/^{86}Sr$ in the Ordovician, with particular attention to the interval with the highest rates of decreasing values in the Middle to Late Ordovician. Lastly, we discuss possible linkages among $^{87}Sr/^{86}Sr$, tectonics, and sea level.

Primary Seawater $^{87}Sr/^{86}Sr$ Trends in Conodont Apatite

Our results from conodont apatite (Fig. 11) show good agreement with the Ordovician brachiopod data of Shields et al. (2003). For example, both our conodont $^{87}Sr/^{86}Sr$ data from the late Darriwilian McLish Formation in Oklahoma and the brachiopod data from that same formation reported in Shields et al. (2003) are between 0.7086 and 0.7087 (n = 8 for conodonts; n = 5 for brachiopods). A more direct comparison between brachiopod and conodont $^{87}Sr/^{86}Sr$ for a single stratigraphic horizon in the McLish Formation is not possible because of uncertainty in the brachiopod positions within

Geological Society of America Bulletin, published online on 30 June 2014 as doi:10.1130/B31038.1

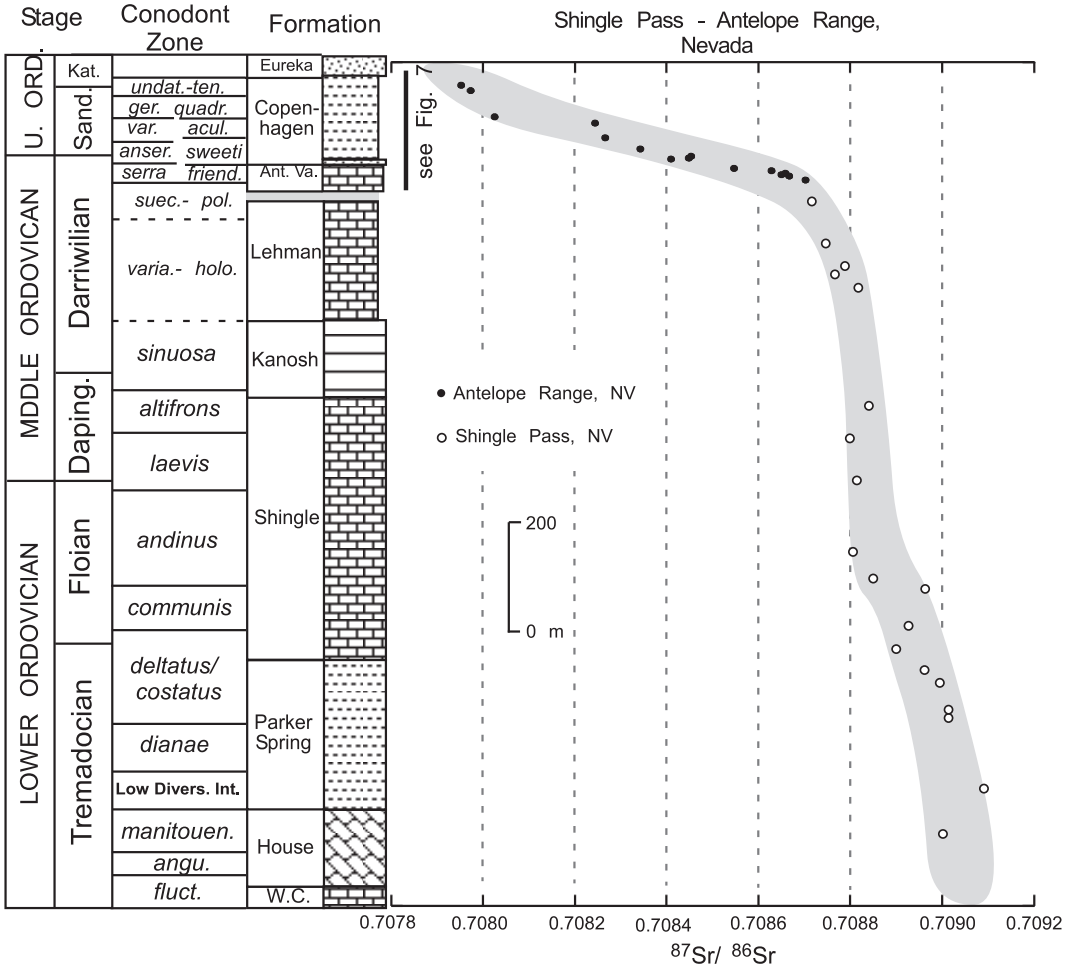

Figure 6. $^{87}Sr/^{86}Sr$ and conodont zones for the Nevada composite, including Shingle Pass (Sweet and Tolbert, 1997) and the Antelope Range (Harris et al., 1979) sections, which are separated by a horizontal gray bar at the top of the Lehman Formation. The Shingle Pass section has previously been studied for $\delta^{13}C$ by Edwards and Saltzman (2014). The Antelope Range was also studied for $\delta^{13}C$ by Saltzman and Young (2005) and for bulk rock $^{87}Sr/^{86}Sr$ by Young et al. (2009) (note that direct comparisons between bulk rock $^{87}Sr/^{86}Sr$ and conodont data is the subject of a separate ongoing study; see Edwards et al., 2013). See Figure 3 and Cooper and Sadler (2012) for list of conodont zone abbreviations used here. Vertical bar near top of figure indicates that these same data from the Antelope Range are plotted in greater detail in Figure 7 in order to show how the $^{87}Sr/^{86}Sr$ line up against actual conodont species ranges. The gray band through the data is generalized (see explanation in Fig. 4 caption), and lithologic symbols used are generalized after Edwards and Saltzman (2014). Ant. Va.—Antelope Valley; W.C.—Whipple Cave. For conodont genera, see Figure 3 caption.

the ~125-m-thick formation (Fig. 4; Shields et al. [2003] indicated five sampling horizons but not the relative spacing between horizons). The Bromide Formation of early Sandbian age in Oklahoma also was studied for conodonts herein and brachiopods in Shields et al. (2003), and although the results are broadly consistent, the drop in seawater $^{87}Sr/^{86}Sr$ within this formation is substantial (from ~0.7085 to 0.7081); this precludes direct comparisons with our data because precise levels in a measured section of the Bromide Formation are not recorded in Shields et al. (2003).

Our conodont apatite-based $^{87}Sr/^{86}Sr$ curve is also broadly similar to the Ordovician compilation curve of McArthur et al. (2012) (Fig. 11, inset), which is based largely on the brachiopod data of Shields et al. (2003) but also includes some bulk rock of Gao and Land (1991), Denison et al. (1998), and Young et al. (2009), and apatite data of Ebneth et al. (2001). Our curve can be directly compared with McArthur et al. (2012) because both curves use the same radiometric age model of Cooper and Sadler (2012). Although the trends between our data and McArthur et al. (2012) compare well, close inspection of the inset in Figure 11 reveals that much of our new conodont apatite $^{87}Sr/^{86}Sr$ reported here is less radiogenic for a given time period (see also Fig. S9 [see footnote 1]). The fact that our data appear less radiogenic overall compared to McArthur et al. (2012) could be an artifact of systematic differences in how individual samples were assigned ages using biostratigraphy or could reflect real differences in how conodonts preserve seawater $^{87}Sr/^{86}Sr$ compared to brachiopods and bulk rock. The concentrations of Sr (ppm) in conodont apatite analyzed for our study were generally high,

Geological Society of America Bulletin, published online on 30 June 2014 as doi:10.1130/B31038.1

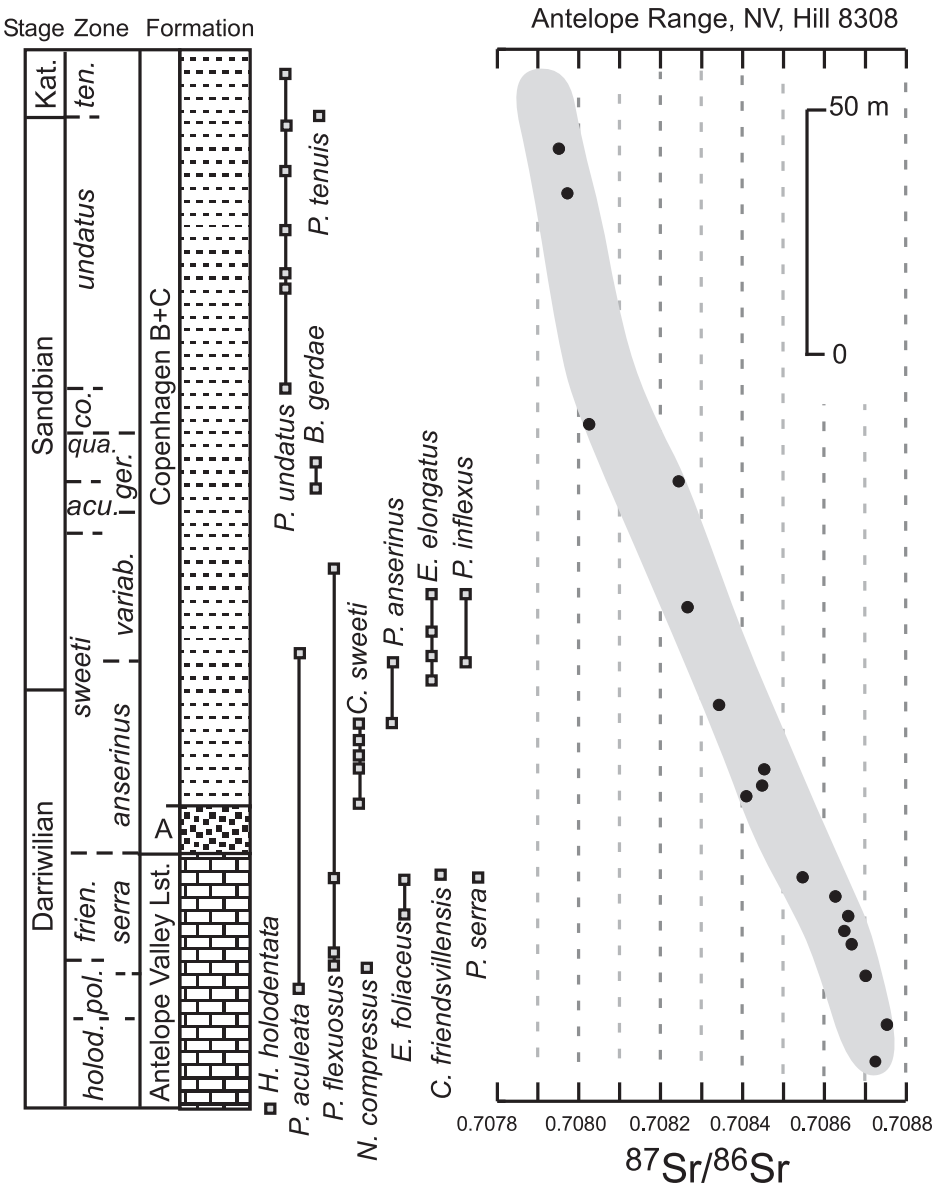

Figure 7. $^{87}Sr/^{86}Sr$ for the Antelope Range section in Nevada (see filled circles in Fig. 6) together with conodont species range data (individual horizons indicated by filled squares; see Harris et al., 1979; Sweet et al., 2005). (Note that the bottom two samples in the *H. holodentata* conodont zone in this figure are not included in the composite in Figure 6, which represents stacking of the two sections at a datum within the *P. polonicus* zone.) See Figure 3 and Cooper and Sadler (2012) for list of conodont zone abbreviations used here. Measured section from Harris et al. (1979) shows the transition from limestone to sandstone at the base of the Copenhagen Formation (Member A) and then back to shaly limestone (see also Saltzman and Young [2005] and Young et al. [2009] for $\delta^{13}C$ and bulk rock $^{87}Sr/^{86}Sr$ studies, respectively). The gray band through the data and lithologic symbols used are generalized (see complete explanation in Fig. 4 caption). For conodont genera, see Figure 3 caption.

with an average of 11,248 ppm (1σ s.d. 5781; Fig. S8 [see footnote 1]), which is roughly an order of magnitude greater than concentrations reported for brachiopods (Shields et al., 2003) or bulk rock (Gao and Land, 1991; Young et al., 2009). It has previously been recognized that Sr concentrations in conodonts are often much greater than expected from a consideration of the Sr partition coefficient in biogenic apatite (and much higher than the Sr concentrations in living marine fish teeth today; see Holmden et al., 1996), which likely reflects that fact that most of the Sr in the conodont apatite is incorporated postmortem, at the sediment-water interface, and during early diagenesis. As suggested by Holmden et al. (1996), if the high concentrations of Sr incorporated into apatite during early and late diagenesis are derived originally from seawater (i.e., from carbonate dissolution/recrystallization processes as opposed to diffusion of radiogenic Sr from shale or clay-rich successions), this will serve to safeguard the integrity of the seawater $^{87}Sr/^{86}Sr$ signature in the conodont during later diagenesis by making it more difficult for deep basinal fluids to alter the $^{87}Sr/^{86}Sr$ ratio (for study of fish teeth, see also Martin and Scher, 2004).

Beyond addressing the accuracy of our conodont apatite-based data by comparison to the seawater $^{87}Sr/^{86}Sr$ brachiopod curve of Shields et al. (2003) and the compilation of McArthur et al. (2012), it is also important to compare the $^{87}Sr/^{86}Sr$ precision as determined by our investigation of sample reproducibility. For the 24 replicate conodont samples we analyzed, the average difference was 4.0×10^{-5}, and the standard deviation (1σ) was 3.1×10^{-5} (Table S4 [see footnote 1]). This average difference of 4.0×10^{-5} is consistent with the reproducibility estimated for brachiopods (e.g., Diener et al., 1996), which may be limited by geological factors related to sample preservation and preparation (as opposed to the analytical uncertainties, which are typically smaller and limited by how precisely a standard can be measured; see Fig. S1 [see footnote 1]).

In summary, although our methods attempted to minimize sources of scatter in the data by extracting conodonts from carbonate rocks, chemical pretreatment of conodont elements, and preference for conodont elements with small amounts of base material and relatively low CAI where possible, future Ordovician studies may continue to refine these methods and potentially achieve accurate and precise results on par with Mesozoic and Cenozoic studies (i.e., ~2.0×10^{-5} for the width of the band of data defining the seawater curve; Farrell et al., 1995).

Ordovician Sr Isotope Stratigraphy and Stratigraphic Resolution

For parts of the Ordovician in which rates of change in $^{87}Sr/^{86}Sr$ are relatively high (~5.0–10.0×10^{-5} per m.y.), Sr isotope stratigraphy is likely to be useful as a high-resolution tool for correlation that is on par with, or potentially better than, conodont biostratigraphy. Sr isotope stratigraphy can also be particularly useful in strata that only preserve long-ranging conodonts or species that have poorly constrained age ranges, such as those at the Clear Spring section (Fig. 9), where there are low yields of shallow-

Geological Society of America Bulletin, published online on 30 June 2014 as doi:10.1130/B31038.1

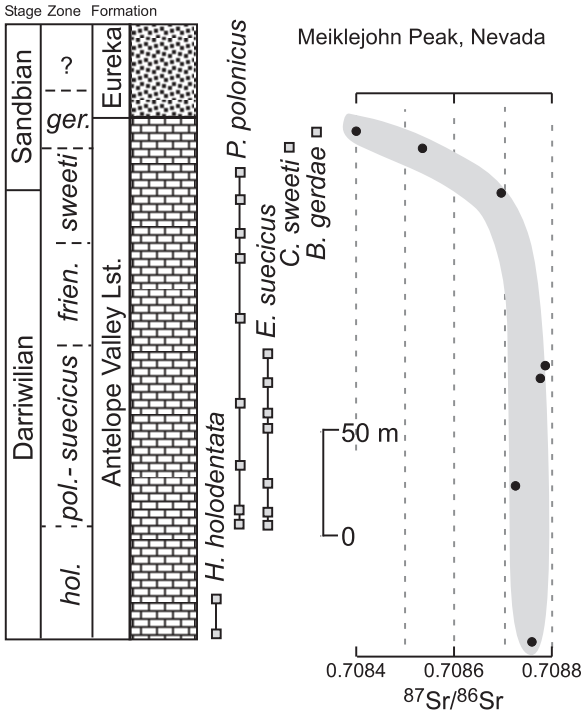

Figure 8. $^{87}Sr/^{86}Sr$ for the Meiklejohn Peak section in Nevada together with conodont species range data (individual horizons indicated by filled squares; see Harris et al., 1979; Sweet et al., 2005). See Figure 3 and Cooper and Sadler (2012) for list of conodont zone abbreviations used here. The gray band through the data and lithologic symbols used are generalized (see complete explanation in Fig. 4 caption). For conodont genera, see Figure 3 caption.

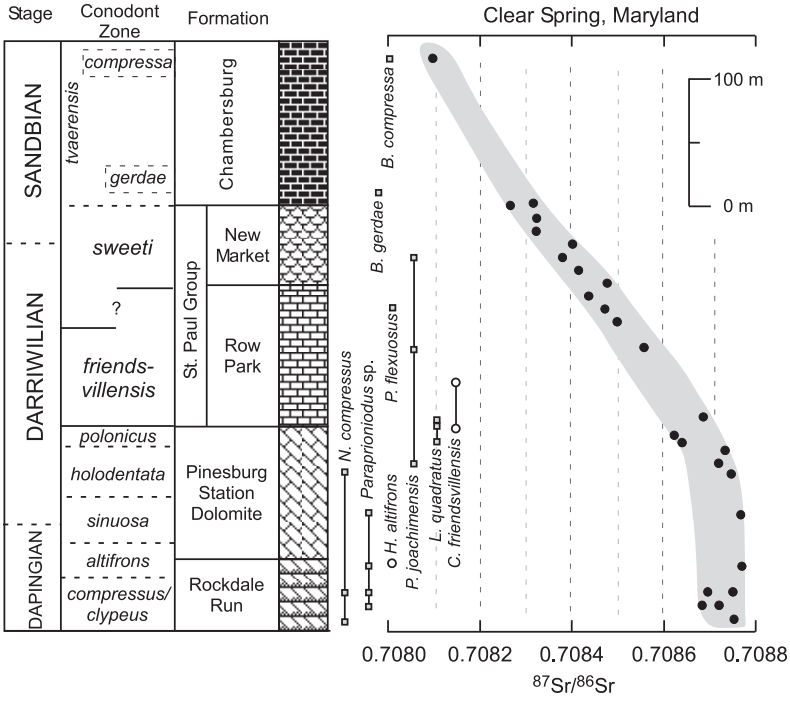

Figure 9. $^{87}Sr/^{86}Sr$ for the Clear Spring section in Maryland together with conodont species range data (individual horizons indicated by filled squares; Leslie et al., 2013). Two key conodont species from nearby sections are included in the range charts and indicated by open circles (see Boger, 1976; Brezinski et al., 1999; note that only the upper part of the Rockdale Run is preserved at Clear Spring). See Figure 3 and Cooper and Sadler (2012) for list of conodont zones used. The gray band through the data and lithologies are generalized (see complete explanation in Fig. 4 caption). For conodont genera, see Figure 3 caption.

water Midcontinent realm conodonts in tidal to shallow subtidal facies. Stratigraphic resolution using $^{87}Sr/^{86}Sr$ analyses of conodonts is limited by sample precision, and, as discussed earlier, our samples run in duplicate are on average different by 4.0×10^{-5} with a 2σ standard deviation of 6.2×10^{-5} (Table S4 [see footnote 1]). Thus, if duplicate or stratigraphically adjacent samples are analyzed, it may be possible in the best case scenario to subdivide parts of the Ordovician into Sr isotope "slices" of ~0.5–1.0 m.y. resolution (i.e., during a 1 m.y. time period in which $^{87}Sr/^{86}Sr$ changed by 8.0×10^{-5}, it may be possible to resolve two distinct 0.5 m.y. intervals; see Table 1; Fig. 12). The Ordovician absolute time scale (Cooper and Sadler, 2012) and relative positioning of samples from different regions within individual conodont zones are also sources of error in Sr isotope stratigraphy. In the discussion that follows, we compare rates of change and potential resolution using Sr isotope stratigraphy through the Ordovician while highlighting key sources of uncertainty in radiometric ages and biostratigraphy (see also GSA Data Repository text [see footnote 1]).

The resolution of Sr isotope stratigraphy in Lower Ordovician stages (Tremadocian–Floian) is relatively low based on a $^{87}Sr/^{86}Sr$ rate of fall of $\sim 1.6 \times 10^{-5}$ per m.y. (Table 1; Figs. 11 and 12; note that some potential structure on this overall fall may be substantiated with future work), which is similar to other slowly changing time periods in the Phanerozoic such as the early Cenozoic (Fig. 1B). For the Middle Ordovician Dapingian Stage, $^{87}Sr/^{86}Sr$ falls from 0.70880 to 0.70875, and the rate of change of 1.9×10^{-5} per m.y. is similar to the Lower Ordovician. The possibility of an older age for the base of the Dapingian at 473 Ma (Thompson and Kah, 2012; Thompson et al., 2012) would further lower the rate of $^{87}Sr/^{86}Sr$ change. Even if we place the top of the Dapingian at 0.70870 in the $^{87}Sr/^{86}Sr$ curve, which is possible resulting from uncertainty in biostratigraphy (i.e., the Dapingian-Darriwilian boundary falls somewhere within the *H. sinuosa* conodont zone), the rate of change goes up, but the resolving power using Sr isotope stratigraphy is still no better than conodont zones (Table 1).

The Middle Ordovician Darriwilian Stage represents a critical time period in which the rate of fall in $^{87}Sr/^{86}Sr$ steepens significantly. Assuming an $^{87}Sr/^{86}Sr$ value of 0.70875 for the base of the Darriwilian and 0.70835 for the top (within the *C. sweeti* zone; Figs. 11 and 12), the rate of change is 4.5×10^{-5} per m.y. (similar to parts of the late Cenozoic; Fig. 1B). Radiometric age dates (Thompson et al., 2012) raise the possibility that the base of the Darriwilian could be as old as 469 Ma, lowering the rate of change

Geological Society of America Bulletin, published online on 30 June 2014 as doi:10.1130/B31038.1

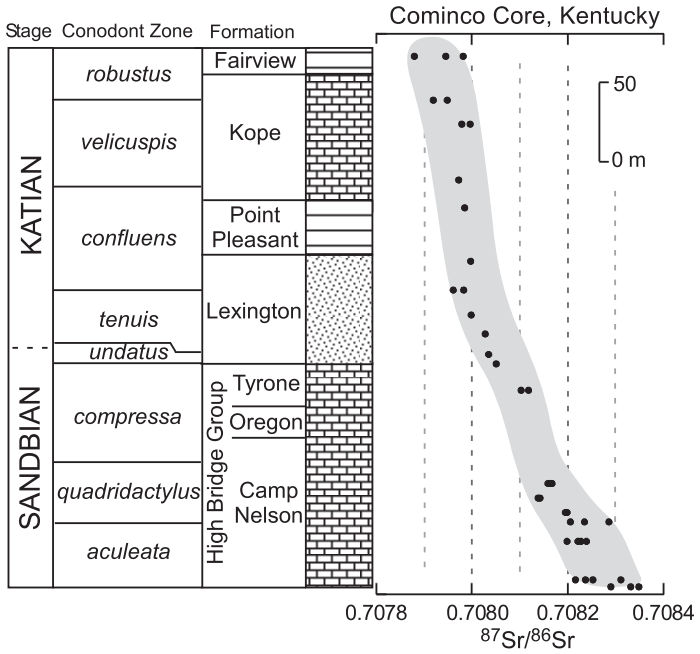

Figure 10. $^{87}Sr/^{86}Sr$ for the Cominco core in Kentucky (see Dwyer, 1996). For details of conodont biostratigraphy, see Sweet (1984) and references therein. The gray band through the data and lithologic symbols used are generalized (see complete explanation in Fig. 4 caption). For conodont genera, see Figure 3 caption.

to 3.5×10^{-5} per m.y. (note that ages for the middle and top of the Darriwilian seem unlikely to move by more than 1–2 m.y. based on dates in Sell et al., 2011). In the Late Ordovician Sandbian Stage, $^{87}Sr/^{86}Sr$ changes from 0.70835 to 0.70800, and the calculated rate of change at 6.5×10^{-5} per m.y. is higher than the preceding Darriwilian.

Rates of $^{87}Sr/^{86}Sr$ change calculated for individual conodont zones in the Darriwilian and Sandbian Stages in some cases greatly exceed the averages (Table 1) and are on par with some of the highest rates in the Phanerozoic such as the late Cenozoic, Middle Jurassic, or Early Triassic (Fig. 1; McArthur et al., 2012). The middle Darriwilian *E. suecicus* zone and partly time-equivalent *P. polonicus* zone yield rates of change of 7.9×10^{-5} and 10.5×10^{-5} per m.y., respectively. However, although the rates of change appear to be elevated significantly by the middle Darriwilian, the number of $^{87}Sr/^{86}Sr$ data points used to calibrate both of the aforementioned zones is still quite limited (three data points at Meiklejohn Peak in Nevada for the *E. suecicus* zone; and a single data point at Meiklejohn Peak and two data points in Oklahoma for the *P. polonicus* zone; Figs. 5 and 8).

In the late Darriwilian *P. serra* zone, the $^{87}Sr/^{86}Sr$ rate of change is 6.5×10^{-5} per m.y. The top of this zone is particularly well calibrated to the $^{87}Sr/^{86}Sr$ curve because the evolutionary transition to *P. anserinus* is captured at Marble Hollow in Tennessee (Fig. 11; Fig. S4 [see footnote 1]). The late Darriwilian *C. friendsvillensis* zone yields a higher rate of change of 8.9×10^{-5} per m.y. However, the $^{87}Sr/^{86}Sr$ calibration for the top of the *C. friendsvillensis* zone is less certain because it includes horizons in Oklahoma that span the ranges of *C.* n. sp. and *C. directus* (Fig. 5), highlighting the importance of taxonomic definitions for zonal boundaries in continuous lineages. In the late Darriwilian to early Sandbian *P. anserinus* and *C. sweeti* zones, the $^{87}Sr/^{86}Sr$ rates of change are 7.8×10^{-5} and 4.4×10^{-5} per m.y., respectively (Table 1), although again uncertainty persists regarding the first appearance datum of *P. anserinus* (e.g., in the Antelope Range of Nevada; see Harris et al. [1979] versus Sweet et al. [2005]) and the lack of evidence for precise placement of the top of the *C. sweeti* zone in most sections (defined by the first occurrence of *P. aculeata*).

In the middle Sandbian *B. variabilis* zone, the $^{87}Sr/^{86}Sr$ rate of change remains high at 6.0×10^{-5} per m.y. The $^{87}Sr/^{86}Sr$ data directly from stratigraphic horizons yielding conodonts of the *B. variabilis* zone are absent in our study, but *E. elongatus* is used as a proxy for this zone. The $^{87}Sr/^{86}Sr$ value used for the top of the *B. variabilis* zone is problematic due to taxonomic uncertainty over early forms of *B. gerdae* (Harris et al., 1979) that define the base of the overlying zone (and base of stage slice Sa2; Bergström et al., 2009). The middle Sandbian *P. aculeata* zone yields the highest rate of change for the entire Ordovician of 18.3×10^{-5} per m.y. (Table 1), but this must be further scrutinized in the context of uncertainty over the taxonomy of *P. aculeata* s.s. and s.l. (e.g., Boger, 1976). Rates of change in $^{87}Sr/^{86}Sr$ slow dramatically in the late Sandbian through the Katian Stages until the curve reverses course and begins to rise somewhere in the upper part of the Katian through the terminal Ordovician Hirnantian Stage.

Tectonics, Sea Level, and the Mid-Darriwilian High Rate of $^{87}Sr/^{86}Sr$ Decrease

As a result of uncertainties in the Ordovician time scale, the question of whether the increased rate of $^{87}Sr/^{86}Sr$ change beginning in the mid-Darriwilian *P. polonicus–P. serra* zone interval represents a significant geologic event in the context of the Phanerozoic remains unclear. (A similar debate over whether a unique geologic event is required to explain the $^{87}Sr/^{86}Sr$ curve for the Early Jurassic was reviewed by Waltham and Gröcke [2006] and McArthur and Wignall [2007].) Both Shields et al. (2003) and Young et al. (2009) suggested that tectonic changes, including plate convergence associated with the Taconic uplift in eastern Laurentia, would have resulted in exposure and erosion of relatively young volcanic and igneous rocks with lower $^{87}Sr/^{86}Sr$. Young et al. (2009) modeled the influence of this weathering event on CO_2 drawdown and found that rates of volcanic degassing may have kept CO_2 levels and climate stable until the late Katian. Sea-level change was not included in this model but exerts an important control on strontium fluxes to the oceans, as detailed in Shields et al. (2003). Because of heterogeneity in continental crust, rises and falls in sea level can change the type and age of rock exposed to weathering on the continents, which may affect the $^{87}Sr/^{86}Sr$ of the riverine Sr flux and also its magnitude. In addition, sea level is sometimes used as a proxy for rates of seafloor spreading, which can affect the relatively nonradiogenic seawater Sr flux from mid-ocean-ridge hydrothermal alteration (Veizer, 1989). Thus, periods of rising sea level might be expected to coincide with an increase in the ratio of nonradiogenic Sr derived from mid-ocean ridges relative to radiogenic Sr weathered from the continents. Here, we examine more closely the evidence showing that the increased rate of $^{87}Sr/^{86}Sr$ fall beginning in the middle Darriwilian *P. polonicus–P. serra* interval coincided with a rise in sea level.

Geological Society of America Bulletin, published online on 30 June 2014 as doi:10.1130/B31038.1

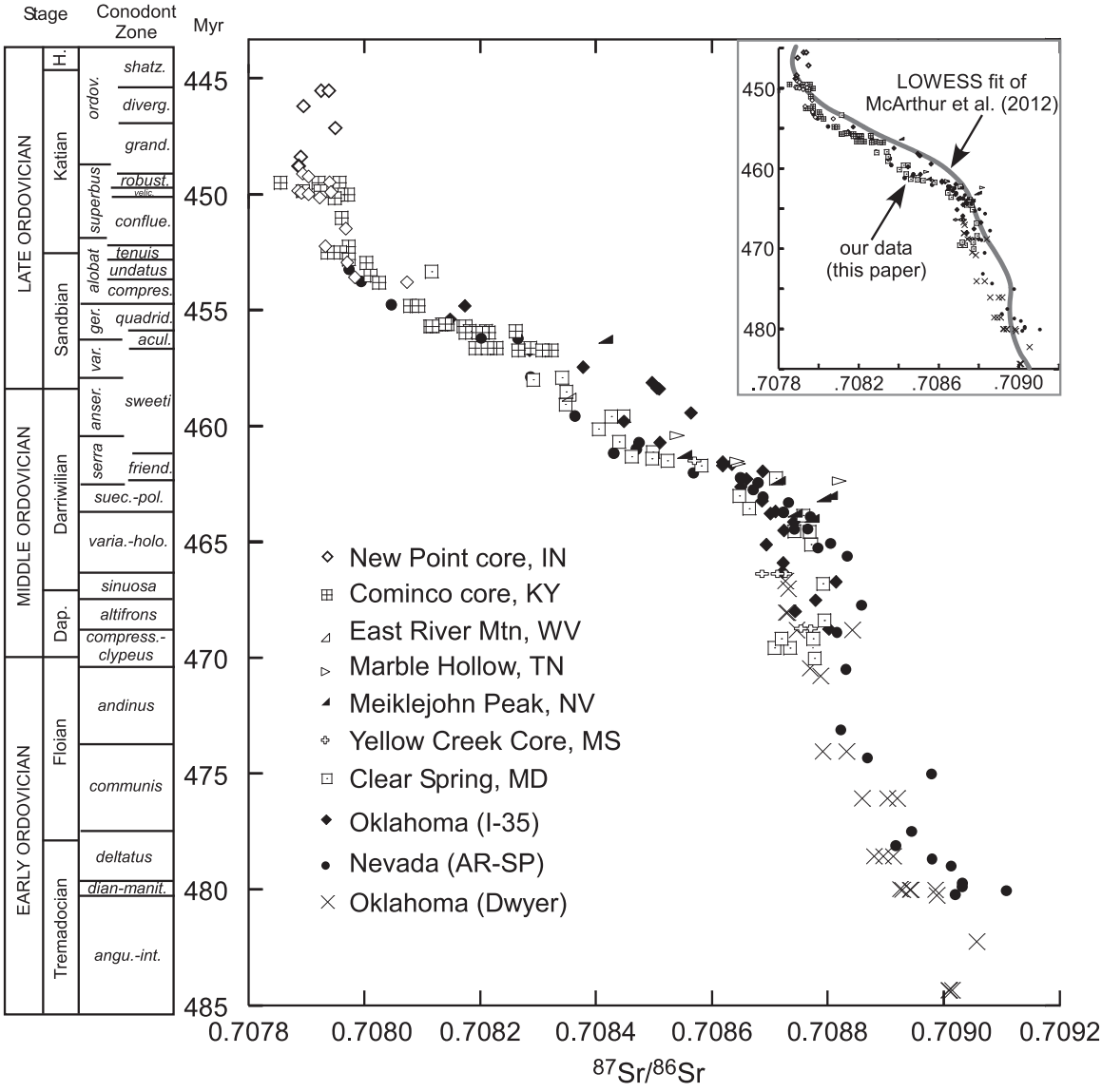

Figure 11. $^{87}Sr/^{86}Sr$ trend for all our sections studied (see Figs. 4–10; Figs. S3–S7 [see text footnote 1]), calibrated to the *Geologic Time Scale 2012* (Cooper and Sadler, 2012). Inset shows the LOWESS fit curve for the Ordovician from McArthur et al. (2012) (see Fig. 1) plotted over our data, both of which are calibrated to the same age model of Cooper and Sadler (2012) and thus are directly comparable. Note that our data are corrected to a preferred value for SRM 987 standard of 0.710245 (see text for discussion and GSA Data Repository Tables S1 and S3 [see text footnote 1]), which is indistinguishable (at the scale of this figure) from McArthur et al. (2012), who used 0.710248. The fact that much of our data is less radiogenic for a given time period compared to McArthur et al. (2012) could be a result of systematic differences in how individual samples were assigned ages using biostratigraphy or could reflect real differences in how conodonts and brachiopods preserve seawater $^{87}Sr/^{86}Sr$. For conodont genera, see Figure 3 caption.

In North America, a prominent Ordovician megasequence (first-order) boundary occurs at the transition between the Sauk and Tippecanoe sequences, which apparently formed over a protracted period of time representing almost the entire Middle Ordovician (e.g., Finney et al., 2007; Morgan, 2012). The global significance of the Sauk-Tippecanoe megasequence boundary may be indicated by relatively low sea level in the Dapingian and Darriwilian Stages elsewhere in the world, with a prominent lowstand recognized in the mid-Darriwilian in some locations (Nielsen, 2004; Su, 2007; Kanygin et al., 2010; Dronov et al., 2011). In North America, maximum regression associated with the Sauk-Tippecanoe megasequence boundary occurred somewhere in the middle Darriwilian and may be narrowed down to the *H. holodentata* conodont zone where biostratigraphic control is particularly good (Dwyer and Repetski, 2012). Few regions in North America contain sections with continuous sedimentation through the Sauk-Tippecanoe transition, but the *H. holodentata* conodont zone and surrounding middle Darri-

Geological Society of America Bulletin, published online on 30 June 2014 as doi:10.1130/B31038.1

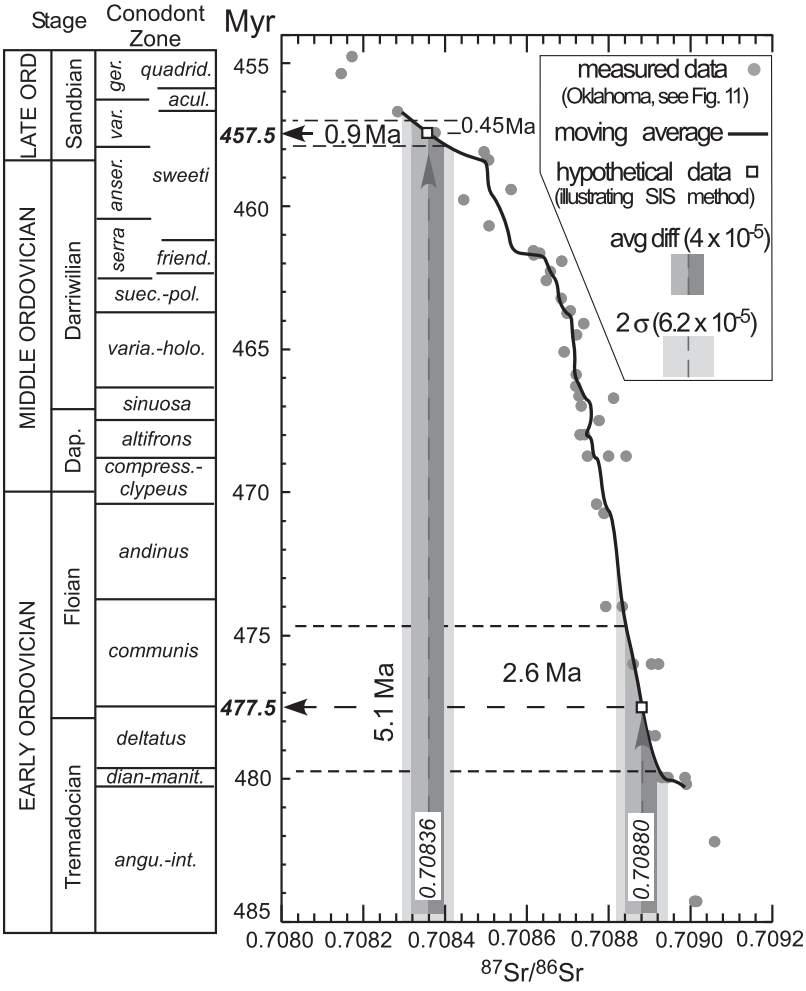

Figure 12. Arbuckle Mountains, Oklahoma, $^{87}Sr/^{86}Sr$ data (gray circles; see Figs. 4, 5, and 11) with a five-point moving average line to illustrate how Sr isotope stratigraphy (SIS) may be used by future investigators. Squares indicate hypothetical data points not obtained in this study, but which instead represent two examples of $^{87}Sr/^{86}Sr$ measurements (0.70888 and 0.70836) that may be obtained by future Ordovician investigations. The two example values are chosen at different parts of the Ordovician curve to emphasize the potential resolution possible using Sr isotope stratigraphy at high versus low rates of $^{87}Sr/^{86}Sr$ change. The age of these two samples is determined in two steps: (1) drawing a vertical line from the *x*-axis (dashed lines with arrows) up to meet the five-point moving average, and (2) drawing a horizontal line from the five-point moving average to where it meets the *y*-axis, indicating sample age (477.5 and 457.5 Ma for $^{87}Sr/^{86}Sr$ values obtained of 0.70888 and 0.70836, respectively). The two darker-colored shaded vertical bars bisected by dashed arrow represent $^{87}Sr/^{86}Sr$ error bars of $\pm 4 \times 10^{-5}$ each, which is the average difference for duplicate analyses in our study (see text for discussion; Table 1; Table S4 [see text footnote 1]). The size of the uncertainty on the age estimate (*y*-axis) is determined by where the edges of these bars intersect the $^{87}Sr/^{86}Sr$ line (moving average). In the best-case scenario, in which a duplicate analysis is run, only one of the $^{87}Sr/^{86}Sr$ error bars of $\pm 4 \times 10^{-5}$ applies, and the uncertainty on the age is minimized (e.g., 2.6 Ma instead of 5.1 Ma, or 0.45 Ma instead of 0.9 Ma). The outer, lightest-colored gray bars represent the 2σ standard deviation based on replicate analyses (see text for discussion and Table S4), which is $\pm 6.2 \times 10^{-5}$, and which increases the uncertainty on the age estimates accordingly (where the outer edges of the light-gray bars hit the $^{87}Sr/^{86}Sr$ moving average line). Note also that the Arbuckle Mountains data are shown separately here from all of our data (Fig. 11) to emphasize the reduced scatter observed when stratigraphic uncertainty (i.e., relative ordering of samples within conodont zones from different regions) is removed or minimized. As in Figure 11, all data are corrected to a preferred value for SRM 987 standard of 0.710245 (see text for discussion and GSA Data Repository Tables S1 and S3 [see text footnote 1]). For conodont genera, see Fig. 3 caption.

wilian zones are present in the sections studied here in Oklahoma and Nevada (the interval is also thought to be complete in Maryland, but conodont element preservation is poor in dolomite).

The Oklahoma and Nevada successions represent excellent opportunities to examine more closely the linkages between $^{87}Sr/^{86}Sr$ and sea level because these regions serve as the reference sections for the Middle Ordovician portion of the Haq and Schutter (2008) Paleozoic global sea-level curve (see also Ross and Ross, 1995; Ross et al., 1989). In east-central Nevada, the Shingle Pass section we analyzed for $^{87}Sr/^{86}Sr$ is comparable to the nearby Ibex area of west-central Utah that was the focus in the study of Haq and Schutter (2008) (see also Miller et al., 2012; Edwards and Saltzman, 2014). A major sequence boundary in Utah occurs in the *P. polonicus–E. suecicus* conodont zones (Haq and Schutter, 2008), which we recognize as near the onset of the increased rates of fall in $^{87}Sr/^{86}Sr$. The next younger depositional sequence occurs in the *P. serra* zone in Oklahoma (Schutter, 1992; Haq and Schutter, 2008) and marks the major change to rising long-term sea level above the Sauk-Tippecanoe megasequence boundary.

Although a causal relationship between sea-level rise and a decrease in $^{87}Sr/^{86}Sr$ in the Darriwilian may exist (i.e., assuming a combination of a reduced riverine flux, which is relatively radiogenic compared to seawater, and an increased hydrothermal flux), different relationships between sea level and $^{87}Sr/^{86}Sr$ are seen in other parts of the Ordovician. For example, following the end-Ordovician (Hirnantian) glaciation, a transition to rising sea level in the Early Silurian coincides with increasing rather than decreasing $^{87}Sr/^{86}Sr$ (Fig. 1). In the Early Ordovician, long-term sea level peaks in the Floian (Munnecke et al., 2010) and then begins to fall, while the $^{87}Sr/^{86}Sr$ shows no obvious change at this time (Figs. 11 and 12; it is possible that higher-resolution $^{87}Sr/^{86}Sr$ data could test whether Sr drops at a modestly slower rate in the Dapingian and early Darriwilian in response to this sea-level fall).

In addition to sea level and associated changes in seafloor spreading, the rate of change in $^{87}Sr/^{86}Sr$ could be influenced by tectonic events on the continents that expose new rock types for weathering. Tectonic events such as the Taconic uplift (Read and Repetski, 2012) and associated changes in weathering (i.e., changes in the ratio of volcanic weathering, mainly basalt, to total silicate weathering) were the preferred explanation by Young et al. (2009) for the Ordovician $^{87}Sr/^{86}Sr$ drop (see also Qing et al., 1998; Shields et al., 2003) and have also been proposed to play an important role in shifts in the Mesozoic and

TABLE 1. ORDOVICIAN Sr ISOTOPE RESOLUTION (Sr ISOTOPE "SLICES") COMPARED TO CONDONT ZONES

Ordovician Stage	Duration (m.y.) GTS 2012	Net drop in $^{87}Sr/^{86}Sr$ ($\times10^{-5}$)	Rate of change in $^{87}Sr/^{86}Sr$ ($\times10^{-5}$ per m.y.)	Number of Sr isotope slices*	Average resolution of Sr slice (m.y.)	Number of conodont zones†	Average resolution of conodont zone (m.y.)
Tremadocian-Floian	15.4	25	1.6	6.3	2.4	9	1.7
Dapingian	2.7	5	1.9	1.3	2.1	3	0.9
Darriwilian	8.9	40	4.5	10	0.9	5	1.8
Sandbian	5.4	35	6.5	8.8	0.6	5	1.1
Katian	7.8	10	1.3	2.5	3.1	7	1.1
Conodont zone (mid-Darriwilian–mid-Sandbian)							
H. holodentata	2.6	5	1.9	1.3	2.0	1	2.6
P. polonicus	1.4	15	10.5	3.8	0.4	1	1.4
E. suecicus	1.3	10	7.9	2.5	0.5	1	1.3
P. serra	2.0	13	6.5	3.3	0.6	1	2.0
C. friendsvillensis	1.1	10	8.9	2.5	0.4	1	1.1
P. anserinus	2.6	20	7.8	5	0.5	1	2.6
C. sweeti	4.5	20	4.4	5	0.9	1	4.5
B. variabilis	1.7	10	6.0	2.5	0.7	1	1.7
P. aculeata	0.8	15	18.3	3.8	0.2	1	0.8

Note: GTS 2012—*Geologic Time Scale 2012* (Cooper and Sadler, 2012). For conodont genera, see Figure 3 caption.

*A Sr "slice" is defined by assuming an error bar (precision) of 4.0×10^{-5}, which is equal to the average difference between duplicate analyses (see Table S4 [text footnote 1] and text for discussion). For example, in the Darriwilian, the net drop in $^{87}Sr/^{86}Sr$ is 40×10^{-5}, and this number divided by precision (4×10^{-5}) yields 10 Sr slices over 8.9 m.y., with an average resolution of 0.9 m.y./slice (see Fig. 12). Note that this represents the best-case scenario and use of the 2σ standard deviation of 6.2×10^{-5} for replicate analyses will result in somewhat coarser resolution. If a sample is not analyzed in duplicate, the error bar is 2 times the precision (which can be based on average difference or 2σ).

†Maximum number using either North Atlantic or North American Midcontinent zonations (Cooper and Sadler, 2012).

Cenozoic (e.g., Richter et al., 1992; McArthur et al., 2001; Waltham and Gröcke, 2006; Kent and Muttoni, 2008). However, it is particularly difficult in the Paleozoic to disentangle the relative roles of sea level and tectonics in exposing or covering rocks of differing ages and $^{87}Sr/^{86}Sr$ on the continents on a global scale (Gouldey et al., 2010; Cramer et al., 2011). Furthermore, because ocean crust is not preserved in the Paleozoic, it is difficult to evaluate the importance of hydrothermal activity related to increased ocean crust production at mid-ocean ridges, which has been linked to large and rapid drops in $^{87}Sr/^{86}Sr$ in the Jurassic and Cretaceous (Jones and Jenkyns, 2001) and potentially the Middle Ordovician (Qing et al., 1998; Shields et al., 2003).

CONCLUSIONS

Although the basic structure of the Ordovician $^{87}Sr/^{86}Sr$ isotope seawater curve is well established and shows continuously falling values, the results of this study using conodont apatite bolster the notion of a significant increase in the rate of fall beginning in the Middle Ordovician (mid-Darriwilian *P. polonicus* to *P. serra* conodont zones). The highest rates of $^{87}Sr/^{86}Sr$ fall at $5.0–10.0 \times 10^{-5}$ per m.y. occur in the mid-Darriwilian to mid-Sandbian (Middle to Late Ordovician). Replicate conodont analyses from the same sample differ by an average of ~4.0×10^{-5} (the 2σ standard deviation is 6.2×10^{-5}), which in the best-case scenario (characterized by the highest rates of fall in $^{87}Sr/^{86}Sr$) allows for subdivision of Ordovician time intervals at a maximum resolution of ~0.5–1.0 m.y. As the density of radiometric age dates increases in the Ordovician with future work, our calibration points based on conodont zones can be continually revised. Changes in global tectonics or sea level are likely causes of the increased rate of fall in $^{87}Sr/^{86}Sr$, although additional modeling studies are needed to determine the magnitude of an event that is required to alter Sr fluxes on the time scales proposed here. Future work should focus on potential implications for the broadly coincident changes in biodiversity (major pulses of the Great Ordovician biodiversification event, GOBE), $\delta^{13}C_{carb}$ (middle Darriwilian isotope carbon excursion, MDICE), temperature, and oxygenation (Kaljo et al., 2007; Trotter et al., 2008; Schmitz et al., 2008, 2010; Ainsaar et al., 2010; Servais et al., 2010; Thompson et al., 2012; Miller, 2012; Harper et al., 2013; Albanesi et al., 2013; Edwards and Saltzman, 2014; Calner et al., 2014). In addition, further refinement of Ordovician $\delta^{13}C$ stratigraphy can also potentially provide improved chemostratigraphic time resolution (e.g., Cramer et al., 2010) when integrated with Sr isotope stratigraphy.

ACKNOWLEDGMENTS

We thank Jeff Linder, Ken Foland, Amanda Howard, and Alexa Sedlacek for help in the Radiogenic Isotope Laboratory at Ohio State University and with sample preparation. Drew Coleman and Paul Fullagar are thanked for training in and access to the Geochronology and Isotope Geochemistry Laboratory at the University of North Carolina–Chapel Hill. We thank Nathaniel Warner and Jennifer Harkness for help in sample preparation at Duke University. Walt Sweet and Ray Ethington provided access to conodont collections. We thank Bryan Sell and Brad Cramer for general discussions of Sr isotope stratigraphy and age dating. Funding was provided in part by National Science Foundation grant EAR-0745452 to Saltzman and EAR-0746181 to Leslie. We thank *GSA Bulletin* Editor Christian Koeberl and Associate Editor Ken MacLeod and two anonymous reviewers for making this a stronger contribution.

REFERENCES CITED

Ainsaar, L., Kaljo, D., Martma, T., Meidla, T., Männik, P., Nõlvak, J., and Tinn, O., 2010, Middle and Upper Ordovician carbon isotope chemostratigraphy in Baltoscandia: A correlation standard and clues to environmental history: Palaeogeography, Palaeoclimatology, Palaeoecology, v. 294, p. 189–201, doi:10.1016/j.palaeo.2010.01.003.

Albanesi, G.L., Bergström, S.M., Schmitz, B., Serra, F., Feltes, N.A., Voldman, G.G., and Ortega, G., 2013, Darriwilian (Middle Ordovician) $\delta^{13}C_{carb}$ chemostratigraphy in the Precordillera of Argentina: Documentation of the middle Darriwilian Isotope carbon excursion (MDICE) and its use for intercontinental correlation: Palaeogeography, Palaeoclimatology, Palaeoecology, v. 389, p. 48–63, doi:10.1016/j.palaeo.2013.02.028.

Azmy, K., Veizer, J., Wenzel, B., Bassett, M.G., and Copper, P., 1999, Silurian strontium isotope stratigraphy: Geological Society of America Bulletin, v. 111, p. 475–483, doi:10.1130/0016-7606(1999)111<0475:SSIS>2.3.CO;2.

Banner, J.L., 2004, Radiogenic isotopes: Systematics and applications to earth surface processes and chemical stratigraphy: Earth-Science Reviews, v. 65, p. 141–194, doi:10.1016/S0012-8252(03)00086-2.

Bauer, J.A., 1983, Conodonts and Conodont Biostratigraphy of the McLish and Tulip Creek Formations of South-Central Oklahoma [M.S. thesis]: Columbus, Ohio, The Ohio State University, 131 p.

Bauer, J.A., 1987a, Conodont Biostratigraphy, Correlation, and Depositional Environments of Middle Ordovician Rocks in Oklahoma [Ph.D. dissertation]: Columbus, Ohio, The Ohio State University, 346 p.

Bauer, J.A., 1987b, Conodonts and Conodont Biostratigraphy of the McLish and Tulip Creek Formations (Middle Ordovician) of South-Central Oklahoma: Oklahoma Geological Survey Bulletin 141, 58 p.

Bauer, J.A., 1989, Conodont biostratigraphy and paleoecology of Middle Ordovician rocks in eastern Oklahoma: Journal of Paleontology, v. 63, p. 92–107.

Bauer, J.A., 1990, Stratigraphy and conodont biostratigraphy of the Upper Simpson Group, Arbuckle Mountains, Oklahoma, *in* Ritter, S.M., ed., Early to Middle Paleozoic Conodont Biostratigrapy of the Arbuckle Mountains southern Oklahoma: Oklahoma Geological Survey Guidebook, v. 27, p. 39–53.

Bauer, J.A., 1994, Conodonts from the Bromide Formation (Middle Ordovician), south-central Oklahoma: Journal of Paleontology, v. 68, p. 358–376.

Bauer, J.A., 2010, Conodonts and Conodont Biostratigraphy of the Joins and Oil Creek Formations, Arbuckle Mountains, South-Central Oklahoma: Oklahoma Geological Survey Bulletin 150, 44 p.

Bergström, S.M., 1971, Conodont biostratigraphy of the Middle and Upper Ordovician of Europe and eastern North America, *in* Sweet, W.C., and Bergström, S.M., eds., Symposium on Conodont Biostratigraphy: Geological Society of America Memoir 127, p. 83–164.

Bergström, S.M., 1973, Biostratigraphy and facies relations in the lower Middle Ordovician of easternmost Tennessee: American Journal of Science, v. 273-A, p. 261–293.

Bergström, S.M., 1986, Biostratigraphic integration of Ordovician graptolite and conodont zones—A regional review, *in* Hughes, C.P., and Richards, R.B., eds., Palaeoecology and Biostratigraphy of Graptolites: Geological Society of London Special Publication 20, p. 61–78.

Bergström, S.M., Chen, X., Gutiérrez-Marco, J.C., and Dronov, A., 2009, The new chronostratigraphic classification of the Ordovician System and its relations to major regional series and stages and to $\delta^{13}C$ chemostratigraphy: Lethaia, v. 42, p. 97–107, doi:10.1111/j.1502-3931.2008.00136.x.

Bertram, C.J., Elderfield, H., Aldridge, R.J., and Conway Morris, S., 1992, $^{87}Sr/^{86}Sr$, $^{143}Nd/^{144}Nd$, and REEs in Silurian phosphatic fossils: Earth and Planetary Science Letters, v. 113, p. 239–249, doi:10.1016/0012-821X(92)90222-H.

Boger, J.B., 1976, Conodont Biostratigraphy of the Upper Beekmantown Group and the St. Paul Group (Middle Ordovician) of Maryland and West Virginia [M.S. thesis]: Columbus, Ohio, The Ohio State University, 360 p.

Brand, U., Posenato, R., Came, R., Affek, H., Angiolini, L., Amzy, K., and Farabegoli, E., 2012, The end-Permian mass extinction: A rapid volcanic CO_2 and CH_4-climatic catastrophe: Chemical Geology, v. 322, p. 121–144, doi:10.1016/j.chemgeo.2012.06.015.

Brezinski, D.K., 1996, Carbonate Ramps and Reefs: Paleozoic Stratigraphy and Paleontology of Western Maryland: Maryland Geological Survey Geologic Guidebook 6, 25 p.

Brezinski, D.K., Repetski, J.E., and Taylor, J.F., 1999, Stratigraphic and paleontologic record of the Sauk III regression in the central Appalachians, *in* Santucci, V.L., and McClelland, L., eds., Stratigraphic and Paleontologic Record of the Sauk III Regression in the Central Appalachians: National Park Service Paleontological Research Technical Report 4, p. 32–41.

Brezinski, D.K., Taylor, J.F., and Repetski, J.E., 2012, Sequential development of platform to off-platform facies of the great American carbonate bank in the central Appalachians, *in* Derby, J.R., Fritz, R.D., Longacre, S.A., Morgan, W.A., and Sternback, C.A., eds., The Great American Carbonate Bank: The Geology and Economic Resources of the Cambrian-Ordovician Sauk Megasequence of Laurentia: American Association of Petroleum Geologists Memoir 98, p. 383–420.

Burke, W.H., Denison, R.E., Hetherington, E.A., Koepnick, R.B., Nelson, H.F., and Otto, J.B., 1982, Variation of seawater $^{87}Sr/^{86}Sr$ throughout Phanerozoic time: Geology, v. 10, p. 516–519, doi:10.1130/0091-7613(1982)10<516:VOSSTP>2.0.CO;2.

Calner, M., Lehnert, O., Wu, R., Dahlqvist, P., and Joachimski, M.M., 2014, $\delta^{13}C$ chemostratigraphy in the Lower-Middle Ordovician succession of Öland (Sweden) and the global significance of the MDICE: GFF, v. 136, no. 1, p. 48–54, doi:10.1080/11035897.2014.901409.

Cooper, R.A., and Sadler, P.M., 2012, The Ordovician Period, *in* Gradstein, F.M., Ogg, J.G., Schimtz, M.D., and Ogg, G.M., eds., The Geologic Time Scale 2012: Amsterdam, Elsevier, p. 489–523.

Cramer, B.D., Loydell, D.K., Samtleben, C., Munnecke, A., Kaljo, D., Männik, P., Martma, T., Jeppsson, L., Kleffner, M.A., Barrick, J.E., Johnson, C.A., Emsbo, P., Joachimski, M.M., Bickert, T., and Saltzman, M.R., 2010, Testing the limits of Paleozoic chronostratigraphic correlation via high-resolution (<500 kyr) integrated conodont, graptolite, and carbon isotope ($\delta^{13}C_{carb}$) biochemostratigraphy across the Llandovery–Wenlock (Silurian) boundary: Is a unified Phanerozoic timescale achievable?: Geological Society of America Bulletin, v. 122, p. 1700–1716, doi:10.1130/B26602.1.

Cramer, B.D., Munnecke, A., Schofield, D.I., Haase, K.M., and Haase-Schramm, A., 2011, A revised $^{87}Sr/^{86}Sr$ curve for the Silurian: Implications for global ocean chemistry and the Silurian timescale: The Journal of Geology, v. 119, p. 335–349, doi:10.1086/660117.

Cummins, D.I., and Elderfield, H., 1994, The strontium isotopic composition of Brigantian (late Dinantian) seawater: Chemical Geology, v. 118, p. 255–270.

Davis, A.C., Bickle, M.J., and Teagle, D.A.H., 2003, Imbalance in the oceanic strontium budget: Earth and Planetary Science Letters, v. 211, p. 173–187, doi:10.1016/S0012-821X(03)00191-2.

Denison, R.E., Koepnick, R.B., Burke, W.H., Hetherington, E.A., and Fletcher, A., 1998, Construction of the Cambrian and Ordovician seawater $^{87}Sr/^{86}Sr$ curve: Chemical Geology, v. 152, p. 325–340, doi:10.1016/S0009-2541(98)00119-3.

Derby, J.R., Bauer, J.A., Miller, M.A., Creath, W.B., Repetski, J.E., Dresbach, R.I., Ethington, R.L., Loch, J.D., Stitt, J.H., Sweet, W.C., McHargue, T.R., Taylor, J.F., Miller, J.F., and Williams, M., 1991, Biostratigraphy of the Timbered Hills, Arbuckle, and Simpson Groups, Cambrian and Ordovician, Oklahoma: A review of the correlation tools and techniques available to the explorationist: Oklahoma Geological Survey Circular 92, p. 15–41.

Diener, A., Ebneth, S., Veizer, J., and Buhl, D., 1996, Strontium isotope stratigraphy of the Middle Devonian: Brachiopods and conodonts: Geochimica et Cosmochimica Acta, v. 60, p. 639–652, doi:10.1016/0016-7037(95)00409-2.

Dronov, A.V., Ainsaar, L., Kaljo, D., Meidla, T., Saadre, T., Einasto, R., 2011, Ordovician of Baltoscandia: Facies, sequences, and sea-level changes, *in* Gutiérrez-Marco, J.C., Rábano, I., and Garcia-Bellido, D., eds., Ordovician of the world: Proceedings of the 11th International Symposium on the Ordovician System, Instituto Geológico y Minero de España, v. 14, p. 143–150.

Dufour, E., Holmden, C., Van Neer, W., Zazzo, A., Patterson, W.P., Degryse, P., and Keppens, E., 2007, Oxygen and strontium isotopes as provenance indicators of fish at archaeological sites: The case study of Sagalassos, SW Turkey: Journal of Archaeological Science, v. 34, p. 1226–1239, doi:10.1016/j.jas.2006.10.014.

Dwyer, G.S., 1996, The Origin of the Upper Dolostone (Upper Knox Group, Middle Ordovician), Black Warrior Basin, Subsurface Mississippi, USA [Ph.D. thesis]: Durham, North Carolina, Duke University, 416 p.

Dwyer, G.S., and Repetski, J.E., 2012, The Middle Ordovician Knox unconformity in the Black Warrior Basin, *in* Derby, J.R., Fritz, R.D., Longacre, S.A., Morgan, W.A., and Sternbach, C.A., eds., The Great American Carbonate Bank: The Geology and Economic Resources of the Cambrian–Ordovician Sauk Megasequence of Laurentia: Association of American Petroleum Geologists Memoir 98, p. 345–356.

Ebneth, S., Diener, A., Buhl, D., and Veizer, J., 1997, Strontium isotope systematics of conodonts: Middle Devonian, Eifel Mountains, Germany: Palaeogeography, Palaeoclimatology, Palaeoecology, v. 132, p. 79–96, doi:10.1016/S0031-0182(97)00057-6.

Ebneth, S., Shields, G.A., Veizer, J., Miller, J.F., and Shergold, J.H., 2001, High-resolution strontium isotope stratigraphy across the Cambrian-Ordovician transition: Geochimica et Cosmochimica Acta, v. 65, p. 2273–2292, doi:10.1016/S0016-7037(01)00580-4.

Edwards, C.T., and Saltzman, M.R., 2014, Carbon isotope ($\delta^{13}C_{carb}$) stratigraphy of the Lower–Middle Ordovician (Tremadocian–Darriwilian) in the Great Basin, western United States: Implications for global correlation: Palaeogeography, Palaeoclimatology, Palaeoecology, v. 399, p. 1–20, doi:10.1016/j.palaeo.2014.02.005.

Edwards, C.T., Saltzman, M.R., Leslie, S.A., Bauer, J.A., Bergström, S.M., and Sweet, W.C., 2013, Strontium isotope ($^{87}Sr/^{86}Sr$) stratigraphy of Ordovician conodont apatite and carbonate rock: Implications for preservation of primary seawater chemistry: Geological Society of America Abstracts with Programs, v. 45, no. 7, p. 528.

Elderfield, H., 1986, Strontium isotope stratigraphy: Palaeogeography, Palaeoclimatology, Palaeoecology, v. 57, p. 71–90, doi:10.1016/0031-0182(86)90007-6.

Epstein, A.G., Epstein, J.B., and Harris, L.D., 1977, Conodont Color Alteration—An Index to Organic Metamorphism: U.S. Geological Survey Professional Paper 995, 27 p.

Ethington, R.L., and Clark, D.L., 1981, Lower and Middle Ordovician conodonts from the Ibex area, western Millard County, Utah: Brigham Young University Geology Studies, v. 28, p. 1–155.

Farrell, J.W., Steven, C.C., and Gromet, L.P., 1995, Improved chronostratigraphic reference curve of late Neogene seawater $^{87}Sr/^{86}Sr$: Geology, v. 23, p. 403–406, doi:10.1130/0091-7613(1995)023<0403:ICRCOL>2.3.CO;2.

Finney, S.C., Ethington, R.L., and Repetski, J.E., 2007, The boundary between the Sauk and Tippecanoe Sloss sequences of North America: Acta Palaeontologica Sinica, v. 46, p. 128–134.

Foland, K.A., and Allen, J.C., 1991, Magma sources for Mesozoic anorogenic granites of the White Mountain magma series, New England, USA: Contributions to Mineralogy and Petrography, v. 109, p. 195–211, doi:10.1007/BF00306479.

Gao, G., and Land L.S., 1991, Geochemistry of Cambro-Ordovician Arbuckle limestone, Oklahoma: implications for diagenetic $\delta^{18}O$ alteration and secular $\delta^{13}C$ and $^{87}Sr/^{86}Sr$ variation: Geochimica et Cosmochimica Acta, v. 55, p. 2911–2920.

Gouldey, J.C., Saltzman, M.R., Young, S.A., and Kaljo, D., 2010, Strontium and carbon isotope stratigraphy of the Llandovery (Early Silurian): Implications for tectonics and weathering: Palaeogeography, Palaeoclimatology, Palaeoecology, v. 296, p. 264–275, doi:10.1016/j.palaeo.2010.05.035.

Haq, B.U., and Schutter, S.R., 2008, A chronology of Paleozoic sea-level changes: Science, v. 322, p. 64–68, doi:10.1126/science.1161648.

Harper, D.A.T., Rasmussen, C.M.O., Liljeroth, M., Blodgett, R.B., Candela, Y., Jin, J., Percival, I.G., Rong, J.y., Villas, E., and Zhan, R.b., 2013, Biodiversity, biogeography and phylogeography of Ordovician rhynchonelliform brachiopods, *in* Harper, D.A.T., and Servais, T., eds., Early Palaeozoic Biogeography and Palaeogeography: Geological Society of London Memoir 38, p. 127–144.

Harris, A.G., Bergström, S.M., Ethington, R.L., and Ross, R.J., Jr., 1979, Aspects of Middle and Upper Ordovician conodont biostratigraphy of carbonate facies in Nevada and southeast California and comparison with some Appalachian successions: Brigham Young University Geology Studies, v. 26, p. 7–44.

Hodell, D.A., Mead, G.A., and Mueller, P.A., 1990, Variation in the strontium isotopic composition of seawater (8 Ma to present): Implications for the chemical weathering rates and dissolved fluxes to the oceans: Chemical Geology, v. 80, p. 291–307.

Holmden, C., Creaser, R.A., Muehlenbachs, K., Bergstrom, S.M., and Leslie, S.A., 1996, Isotopic and elemental systematics of Sr and Nd in 454 Ma biogenic apatites: Implications for paleoseawater studies: Earth and Planetary Science Letters, v. 142, p. 425–437, doi:10.1016/0012-821X(96)00119-7.

Horwitz, E.P., Chiarizia, R., and Dietz, M.L., 1992, A novel strontium-selective extraction chromatographic resin: Solvent Extraction and Ion Exchange, v. 10, p. 313–336.

Ingram, B.L., Coccioni, R., Montanari, A., and Richter, F.M., 1994, Strontium isotopic composition of Mid-Cretaceous seawater: Science, v. 264, p. 546–550, doi:10.1126/science.264.5158.546.

Jeppsson, L., and Anehus, R., 1995, A buffered formic acid technique for conodont extraction: Journal of Paleontology, v. 69, p. 790–794.

John, E., Cliff, B., and Wignall, P., 2008, A positive trend in seawater $^{87}Sr/^{86}Sr$ values over the early–middle Frasnian boundary (Late Devonian) recorded in well-preserved conodont elements from the Holy Cross Mountains, Poland: Palaeogeography, Palaeoclimatology, Palaeoecology, v. 269, p. 166–175, doi:10.1016/j.palaeo.2008.04.031.

Jones, C.E., and Jenkyns, H.C., 2001, Seawater strontium isotopes, oceanic anoxic events, and seafloor hydrothermal activity in the Jurassic and Cretaceous: American Journal of Science, v. 301, p. 112–149, doi:10.2475/ajs.301.2.112.

Jones, C.E., Jenkyns, H.C., Coe, A.L., and Hesselbo, S.P., 1994, Strontium isotopic variations in Jurassic and Cretaceous seawater: Geochimica et Cosmochimica Acta, v. 58, p. 3061–3074, doi:10.1016/0016-7037(94)90179-1.

Kaljo, D., Martma, T., and Saadre, T., 2007, Post-Hunnebergian Ordovician carbon isotope trend in Baltoscandia, its environmental implications and some similarities with that of Nevada: Palaeogeography, Palaeoclimatology, Palaeoecology, v. 245, p. 138–155, doi:10.1016/j.palaeo.2006.02.020.

Kanygin, A., Dronov, A., Timokhin, A., and Gonta, T., 2010, Depositional sequences and palaeoceanographic change in the Ordovician of the Siberian craton: Palaeogeography, Palaeoclimatology, Palaeoecology, v. 296, p. 285–296, doi:10.1016/j.palaeo.2010.02.014.

Kent, D.V., and Muttoni, G., 2008, Equatorial convergence of India and early Cenozoic climate trends: Proceedings of the National Academy of Sciences of the United States of America, v. 105, p. 16,065–16,070, doi:10.1073/pnas.0805382105.

Korte, C., Kozur, H.W., Bruckshen, P., and Veizer, J., 2003, Strontium isotope evolution of Late Permian and Triassic seawater: Geochimica et Cosmochimica Acta, v. 67, p. 47–62, doi:10.1016/S0016-7037(02)01035-9.

Korte, C., Kozur, H.W., Joachimski, M.M., Strauss, H., Veizer, J., and Schwark, L., 2004, Carbon, sulfur, oxygen, and strontium isotope records, organic geochemistry, and biostratigraphy across the Permian/Triassic boundary in Abadeh, Iran: International Journal of Earth Sciences, v. 93, p. 565–581.

Korte, C., Jasper, T., Kozur, H.W., and Veizer, J., 2006, $^{87}Sr/^{86}Sr$ record of Permian seawater: Palaeogeography, Palaeoclimatology, Palaeoecology, v. 240, p. 89–107, doi:10.1016/j.palaeo.2006.03.047.

Kürschner, W., Becker, T.H., Buhl, D., and Veizer, J., 1992, Strontium isotopes of conodonts: Devonian/Carboniferous transition in the northern Rhenish Slate Mountains, Germany: Annales de la Société Géologique de Belgique, v. 115, p. 595–623.

Leslie, S.A., and Lehnert, O., 2005, Middle Ordovician (Chazyan) sea-level changes and the evolution of the Ordovician conodont genus *Cahabagnathus* Bergström 1983: Journal of Paleontology, v. 79, p. 1131–1142, doi:10.1666/0022-3360(2005)079[1131:MOCSCA]2.0.CO;2.

Leslie, S.A., Saltzman, M.R., Bergström, S.M., Repetski, J.E., Howard, A., and Seward, A.M., 2011, Conodont biostratigraphy and stable isotope stratigraphy across the Knox/Beekmantown unconformity in the central Appalachians, *in* Gutierrez-Marco, J.C., Rabano, I., and Garcia-Bellido, D., eds., Ordovician of the World: Madrid, Instituto Geológico y Minero de España, Caudernos del Museo Geominero, v. 14, p. 301–308.

Leslie, S.A., Sell, B.K., Saltzman, M.R., Repetski, J.E., and Edwards, C.T., 2012, The East River Mountain K-bentonite bed, a central Appalachian marker that closely approximates the Middle-Upper Ordovician (Darriwilian-Sandbian) boundary: Geological Society of America Abstracts with Programs, v. 44, no. 7, p. 590.

Leslie, S.A., Repetski, J.E., Saltzman, M.R., Kaznosky, C.M., and Lizer, A.M., 2013, Conodont biostratigraphy of the Rockdale Run Formation, Pinesburg Station Dolomite, St. Paul Group, and Chambersburg Formation (Middle to Lower Upper Ordovician) near Clear Spring, Maryland: Geological Society of America Abstracts with Programs, v. 45, no. 7, p. 836.

MacLeod, K.G., Huber, B.T., and Fullagar, P.D., 2001, Evidence for a small (0.000030) but resolvable increase in seawater $^{87}Sr/^{86}Sr$ ratios across the Cretaceous-Tertiary boundary: Geology, v. 29, p. 303–306, doi:10.1130/0091-7613(2001)029<0303:EFASBR>2.0.CO;2.

Martin, E.E., and Macdougall, J.D., 1995, Sr and Nd isotopes at the Permian/Triassic boundary: A record of climate change: Chemical Geology, v. 125, p. 73–99, doi:10.1016/0009-2541(95)00081-V.

Martin, E.E., and Scher, H.D., 2004, Preservation of seawater Sr and Nd isotopes in fossil fish teeth: Bad news and good news: Earth and Planetary Science Letters, v. 220, p. 25–39, doi:10.1016/S0012-821X(04)00030-5.

McArthur, J.M., 1994, Recent trends in strontium isotope stratigraphy: Terra Nova, v. 6, p. 331–358, doi:10.1111/j.1365-3121.1994.tb00507.x.

McArthur, J.M., and Howarth, R.J., 2004, Strontium isotope stratigraphy, *in* Gradstein, F., Ogg, J., and Smith, A., eds., A Geological Time Scale 2004 (1st ed.): Cambridge, UK, Cambridge University Press, p. 96–105.

McArthur, J.M., and Wignall, P.B., 2007, Comment on "Non-uniqueness and interpretation of the seawater $^{87}Sr/^{86}Sr$ curve" by Dave Waltham and Darren R. Gröcke (GCA, 70, 2006, 384–394): Geochimica et Cosmochimica Acta, v. 71, p. 3382–3386, doi:10.1016/j.gca.2006.10.026.

McArthur, J.M., Howarth, R.J., and Bailey, T.R., 2001, Strontium isotope stratigraphy: LOWESS Version 3: Best fit to the marine Sr isotope curve for 0–509 Ma and accompanying look up table for deriving numerical age: The Journal of Geology, v. 109, p. 155–170, doi:10.1086/319243.

McArthur, J.M., Howarth, R.J., and Shields, G.A., 2012, Strontium isotope stratigraphy, *in* Gradstein, F.M., Ogg, J.G., Schmitz, M., and Ogg, G., eds., The Geologic Time Scale 2012: Amsterdam, Elsevier, p. 127–144.

Miller, A.I., 2012, The Ordovician radiation: Macroevolutionary crossroads of the Phanerozoic, *in* Talent, J., ed., Earth and Life: Global Biodiversity, Extinction Intervals and Biogeographic Perturbations through Time: Dordrecht, Netherlands, Springer, p. 381–394.

Miller, J.M., Evans, K.R., Loch, J.D., Ethington, R.L., Stitt, J.H., Holmer, L., and Popov, L.E., 2003, Stratigraphy of the Sauk III interval (Cambrian-Ordovician) in the Ibex area, western Millard County, Utah, and central Texas: Brigham Young University Geology Studies, v. 47, p. 23–118.

Miller, J.M., Evans, K.R., and Dattilo, B.F., 2012, The Great American carbonate bank in the miogeocline of western central Utah: Tectonic influences on sedimentation, *in* Derby, J.R., Fritz, R.D., Longacre, S.A., Morgan, W.A., and Sternbach, C.A., eds., The Great American Carbonate Bank: The Geology and Economic Resources of the Cambrian-Ordovician Sauk Megasequence of Laurentia: Association of American Petroleum Geologists Memoir 98, p. 769–854.

Mitchell, R.W., 1982, Middle Ordovician St. Paul Group, *in* Lyttle, P.T., ed., Central Appalachian Geology: Fieldtrip Guidebook to Combined Northeast-Southeast Meeting of the Geological Society of America: Geological Society of America, p. 175–216.

Mitchell, R.W., 1985, Comparative sedimentology of shelf carbonates of the Middle Ordovician St. Paul Group, central Appalachians: Sedimentary Geology, v. 43, p. 1–41, doi:10.1016/0037-0738(85)90053-3.

Morgan, W.A., 2012, Sequence stratigraphy of the Great American carbonate bank, *in* Derby, J.R., Fritz, R.D., Longacre, S.A., Morgan, W.A., and Sternbach, C.A., eds., The Great American Carbonate Bank: The Geology and Economic Resources of the Cambrian-Ordovician Sauk Megasequence of Laurentia: Association of American Petroleum Geologists Memoir 98, p. 37–79.

Munnecke, A., Calner, M., Harper, D.A.T., and Servais, T., 2010, Ordovician and Silurian sea-water chemistry, sea level, and climate: A synopsis: Palaeogeography, Palaeoclimatology, Palaeoecology, v. 296, p. 389–413, doi:10.1016/j.palaeo.2010.08.001.

Needham, L., 2007, A High Resolution Pennsylvanian–Early Permian Seawater $^{87}Sr/^{86}Sr$ Curve [M.S. thesis]: Boise State University Theses and Dissertations Paper 422 (M. Schmitz, adviser), http://scholarworks.boisestate.edu/td/422.

Neuman, R.B., 1951, St. Paul Group: A revision of the "Stones River" Group of Maryland and adjacent states: Geological Society of America Bulletin, v. 62, p. 267–324, doi:10.1130/0016-7606(1951)62[267:SPGARO]2.0.CO;2.

Nielsen, A.T., 2004, Ordovician Sea level changes: A Baltoscandian perspective, *in* Webby, B.D., Droser, M.L., Paris, F., and Percival, I.G., eds., The Great Ordovician Diversification Event: New York, Columbia University Press, p. 84–93.

Palmer, M.R., and Edmond, J.M., 1989, The strontium isotope budget of the modern ocean: Earth and Planetary Science Letters, v. 92, p. 11–26, doi:10.1016/0012-821X(89)90017-4.

Qing, H., Barnes, C.R., Buhl, D., and Veizer, J., 1998, The strontium isotopic composition of Ordovician and Silurian brachiopods and conodonts: Relationships to geological events and implications for coeval seawater: Geochimica et Cosmochimica Acta, v. 62, p. 1721–1733, doi:10.1016/S0016-7037(98)00104-5.

Read, J.F., and Repetski, J.E., 2012, Cambrian–Lower Middle Ordovician passive carbonate margin, southern Appalachians, *in* Derby, J.R., Fritz, R.D., Longacre, S.A., Morgan, W.A., and Sternbach, C.A., eds., The Great American Carbonate Bank: The Geology and Economic Resources of the Cambrian-Ordovician Sauk Megasequence of Laurentia: Association of American Petroleum Geologists Memoir 98, p. 357–382.

Richter, F.M., Rowley, D.B., and DePaolo, D.J., 1992, Sr isotope evolution of seawater: The role of tectonics: Earth and Planetary Science Letters, v. 109, p. 11–23, doi:10.1016/0012-821X(92)90070-C.

Ross, C.A., and Ross, J.R.P., 1995, North American depositional sequences and correlations, *in* Cooper, J.D., Droser, M.L., and Finney, S.C., eds., Ordovician Odyssey: Proceedings of 7th International Symposium on the Ordovician System: Pacific Section. Fullerton, California, Society for Sedimentary Geology, p. 309–313.

Ross, R.J., Jr., James, N.P., Hintze, L.F., and Poole, F.G., 1989, Architecture and evolution of a Whiterockian (Early Middle Ordovician) carbonate platform, Basin Ranges of western U.S.A., *in* Crevello, P.D., Wilson, J.L., Sarg, J.F., and Read, J.F., eds., Controls on Carbonate Platform and Basin Development: Society of Economic Paleontologists and Mineralogists Special Publication 44, p. 167–185.

Ruppel, S.C., James, E.W., Barrick, J.E., Nowlan, G., and Uyeno, T.T., 1996, High-resolution $^{87}Sr/^{86}Sr$ chemostratigraphy of the Silurian: Implications for event correlation and strontium flux: Geology, v. 24, p. 831–834, doi:10.1130/0091-7613(1996)024<0831:HRSSCO>2.3.CO;2.

Saltzman, M.R., 2005, Phosphorus, nitrogen, and the redox evolution of the Paleozoic oceans: Geology, v. 33, p. 573–576, doi:10.1130/G21535.1.

Saltzman, M.R., and Young, S.A., 2005, A long-lived glaciation in the Late Ordovician?: Isotopic and sequence stratigraphic evidence from western Laurentia: Geology, v. 33, p. 109–112, doi:10.1130/G21219.1.

Sando, W.J., 1957, Beekmantown Group (Lower Ordovician) of Maryland: Geological Society of America Memoir 68, 161 p.

Schmitz, B., Harper, D.A.T., Peucker-Ehrenbrink, B., Stouge, S., Alwmark, C., Cronholm, A., Bergström, S.M., Tassinari, M., and Xiaofeng, W., 2008, Asteroid breakup linked to the Great Ordovician biodiversification event: Nature Geoscience, v. 1, p. 49–53, doi:10.1038/ngeo.2007.37.

Schmitz, B., Bergström, S.M., and Wang, X., 2010, The middle Darriwilian (Ordovician) $\delta^{13}C$ excursion (MDICE) discovered in the Yangtze Platform succession in China; implications of its first recorded occurrence outside Baltoscandia: Journal of the Geological Society of London, v. 167, p. 249–259, doi:10.1144/0016-76492009-080.

Schutter, S.R., 1992, Ordovician hydrocarbon distribution in North America and its relationship to eustatic cycles, *in* Webby, B.D., and Laurie, J.R., eds., Global Perspectives on Ordovician Geology, Proceedings of the Sixth Annual International Symposium on the Ordovician: Sydney, Australia, University of Sydney, p. 421–432.

Sell, B., Leslie, S.A., and Maletz, J., 2011, New U-Pb zircon data for the GSSP for the base of the Katian in Atoka, Oklahoma, USA, and the Darriwilian in Newfoundland, Canada, *in* Gutierrez-Marco, J.C, Rabano, I., and Garcia-Bellido, D., eds., Ordovician of the World: Madrid, Instituto Geológico y Minero de España, Caudernos del Museo Geominero, v. 14, p. 537–546.

Sell, B., Ainsaar, L., and Leslie, S., 2013, Precise timing of the Late Ordovician (Sandbian) supereruptions and

associated environmental, biological, and climatological events: Journal of the Geological Society of London, v. 170, no. 5, p. 711–714, doi:10.1144/jgs2012-148.

Servais, T., Owen, A.W., Harper, D.A.T., Kröger, B., and Munnecke, A., 2010, The Great Ordovician biodiversification event (GOBE): The palaeoecological dimension: Palaeogeography, Palaeoclimatology, Palaeoecology, v. 294, p. 99–119, doi:10.1016/j.palaeo.2010.05.031.

Shields, G.A., Carden, G.A., Veizer, J., Meidla, T., Rong, J., and Li, R., 2003, Sr, C, and O isotope geochemistry of Ordovician brachiopods: A major isotopic event around the Middle-Late Ordovician transition: Geochimica et Cosmochimica Acta, v. 67, p. 2005–2025, doi:10.1016/S0016-7037(02)01116-X.

Su, W., 2007, Ordovician sea-level changes: Evidence from the Yangtze Platform: Acta Palaeontologica Sinica, v. 46, supplement, p. 471–476.

Sweet, W.C., 1984, Graphic correlation of upper Middle and Upper Ordovician rocks, North American Midcontinent Province, U.S.A., *in* Bruton, D.L., ed., Aspects of the Ordovician System: Oslo, Norway, University of Oslo, p. 23–35.

Sweet, W.C., 1995, Graphic assembly of a conodont-based composite standard for the Ordovician System of North America, *in* Mann, K.O., and Lane, H.R., eds., Graphic Correlation: Society for Sedimentary Geology Special Publication 53, p. 139–150.

Sweet, W.C., and Bergström, S.M., 1976, Conodont biostratigraphy of the Middle and Upper Ordovician of the United States Midcontinent, *in* Bassett, M.G., ed., The Ordovician System: Proceedings of a Palaeontological Association Symposium: Birmingham, University of Wales Press, and Cardiff, National Museum of Wales, p. 121–151.

Sweet, W.C., and Bergström, S.M., 1984, Conodont provinces and biofacies of the Late Ordovician, *in* Clark, D.L., ed., Conodont Biofacies and Provincialism: Geological Society of America Special Paper 196, p. 69–88, doi:10.1130/SPE196-p69.

Sweet, W.C., and Tolbert, C.M., 1997, An Ibexian (Lower Ordovician) reference section in the southern Egan Range, Nevada, for a conodont-based chronstratigraphy, *in* Taylor, M.E., ed., Early Paleozoic Biochronology of the Great Basin, Western United States: U.S. Geological Survey Professional Paper 1579, p. 51–84.

Sweet, W.C., Ethington, R.L., and Harris, A.G., 2005, A conodont-based standard reference section in central Nevada for the Lower and Middle Ordovician Whiterockian Series: Bulletins of American Paleontology, v. 369, p. 35–52.

Thompson, C.K., and Kah, L.C., 2012, Sulfur isotope evidence for widespread euxinia and a fluctuating oxycline in Early to Middle Ordovician greenhouse oceans: Palaeogeography, Palaeoclimatology, Palaeoecology, v. 313–314, p. 189–214, doi:10.1016/j.palaeo.2011.10.020.

Thompson, C.K., Kah, L.C., Astini, R., Bowring, S.A., and Buchwaldt, R., 2012, Bentonite geochronology, marine geochemistry, and the Great Ordovician biodiversification event (GOBE): Palaeogeography, Palaeoclimatology, Palaeoecology, v. 321–322, p. 88–101, doi:10.1016/j.palaeo.2012.01.022.

Trotter, J.A., Korsch, M.J., Nicoll, R.S., and Whitford, D.J., 1999, Sr isotopic variation in single conodont elements: Implications for defining the Sr seawater curve, *in* Serpagli, E., ed., Studies on Conodonts. Proceedings of the Seventh European Conodont Symposium 1998: Bolletino della Società Paleontologica Italiana, v. 37, p. 507–514.

Trotter, J.A., Williams, I.S., Barnes, C.R., Lécuyer, C., and Nicoll, R.S., 2008, Did cooling oceans trigger Ordovician biodiversification? Evidence from conodont thermometry: Science, v. 321, p. 550–554, doi:10.1126/science.1155814.

Tucker, R.D., and McKerrow, W.S., 1995, Early Paleozoic chronology: A review in light of new U-Pb zircon ages from Newfoundland and Britain: Canadian Journal of Earth Sciences, v. 32, p. 368–379, doi:10.1139/e95-032.

Twitchett, R.J., 2007, Climate change across the Permian/Triassic boundary, *in* Williams, M., et al., eds., Deep-Time Perspectives on Climate Change: Marrying the Signal from Computer Models and Biological Proxies: London, Geological Society of London, The Micropalaeontological Society Special Publications, p. 191–200.

Van Geldern, R., Joachimski, M.M., Day, J., Jansen, U., Alvarez, F., Yolkin, E.A., and Ma, X.-P., 2006, Carbon, oxygen and strontium isotope records of Devonian brachiopod shell calcite: Palaeogeography, Palaeoclimatology, Palaeoecology, v. 240, p. 47–67, doi:10.1016/j.palaeo.2006.03.045.

Veizer, J., 1989, Strontium isotopes in seawater through time: Annual Review of Earth and Planetary Sciences, v. 17, p. 141–167, doi:10.1146/annurev.ea.17.050189.001041.

Veizer, J., Buhl, D., Diener, A., Ebneth, S., Podlaha, O.G., Bruckschen, P., Jasper, T., Korte, C., Schaaf, M., Ala, D., and Azmy, K., 1997, Strontium isotope stratigraphy: Potential resolution and event correlation: Palaeogeography, Palaeoclimatology, Palaeoecology, v. 132, p. 65–77, doi:10.1016/S0031-0182(97)00054-0.

Votaw, R.B., 1971, Conodont Biostratigraphy of the Black River Group (Middle Ordovician) and Equivalent Rocks of the Eastern Midcontinent, North America [Ph.D. dissertation]: Columbus, Ohio, The Ohio State University, 170 p.

Waltham, D., and Gröcke, D.R., 2006, Non-uniqueness and interpretation of the seawater $^{87}Sr/^{86}Sr$ curve: Geochimica et Cosmochimica Acta, v. 70, p. 384–394, doi:10.1016/j.gca.2005.09.014.

Webby, B.D., Cooper, R.A., Bergström, S.M., and Paris, F., 2004, Stratigraphic framework and time slices, *in* Webby, B.D., Paris, F., Droser, M.L., and Percival, I.G., eds., The Great Ordovician Biodiversification Event: New York, Columbia University Press, p. 41–47.

Woodard, S.C., Thomas, D.J., Grossman, E.L., Olszewski, T.D., Yancey, T.E., Miller, B.V., and Raymond, A., 2013, Radiogenic isotope composition of Carboniferous seawater from North American epicontinental seas: Palaeogeography, Palaeoclimatology, Palaeoecology, v. 370, p. 51–63, doi:10.1016/j.palaeo.2012.11.018.

Young, S.A., Saltzman, M.R., Foland, K., Linder, J., and Kump, L., 2009, A major drop in seawater $^{87}Sr/^{86}Sr$ during the Middle Ordovician (Darriwilian): Links to volcanism and climate?: Geology, v. 37, p. 951–954, doi:10.1130/G30152A.1.

Science Editor: Christian Koeberl
Associate Editor: Kenneth G. MacLeod

Manuscript Received 19 November 2013
Revised Manuscript Received 25 April 2014
Manuscript Accepted 20 May 2014

Printed in the USA